DESIGN OF IMPROVED MICROSTRIP FILTER STRUCTURES

FOR

WIRELESS APPLICATIONS

A thesis submitted towards the partial fulfillment of the requirements for the award of degree of

MASTER OF ENGINEERING

IN

ELECTRONICS AND COMMUNICATION

Submitted by

Ambika Chhabra

Roll. No. 801461003

Under the guidance of

Dr. Rajesh Khanna (Professor, ECED)

DEPARTMENT OF ELECTRONICS AND COMMUNICATION ENGINEERING
THAPAR UNIVERSITY, PATIALA-147004

PUNJAB, INDIA

JULY - 2016

CERTIFICATE AND DECLARATION

I, Ambika Chhabra hereby declare that the work which is being presented in the dissertation entitled **"Design of improved Microstrip Filter Structures for Wireless Applications"** by me in the partial fulfillment of the requirement for the award of degree of Master of Engineering in Electronics and Communication submitted in Electronics and Communication Department of Thapar University, Patiala is an authentic record of my own work carried out under the guidance of **Dr. Rajesh Khanna (Professor)**, Electronics and Communication Engineering Department. The matter presented in this dissertation has not been submitted in any other University/Institute for the award of degree.

Ambika

Date: 29/6/2016

Ambika Chhabra

Roll no. 801461003

This is to certify that the above statement made by the student is correct to the best of my knowledge and belief.

Date: 29/6/2016

Dr. Rajesh Khanna

Professor, ECED

Thapar University

Countersigned by:

Dr. Sanjay Sharma

Professor and Head (ECED)

ECED, Thapar University

Patiala, 147001

Dr. S.S. Bhatia

Dean of academic affairs

Thapar University

Patiala, 147001

ACKNOWLEDGEMENT

This thesis represents not only my keyboard work; it is rather a milestone in more than one year of work at Thapar University and specifically within the Antenna and research Laboratory.

I would have never accomplished in completing my work without the encouragement and help provided to me by different people. I am getting short of words to reveals my deep regards. I take this opportunity to express my subtle sense of gratitude and respect to all those who supported me through thesis duration.

I acknowledge with gratitude and modesty my deficit to **Dr. Rajesh Khanna (Professor)** Electronics & Communication Engineering Department, Thapar University Patiala under whose direction I had the privilege to complete my thesis. I am really very fortunate to have the opportunity to work with them.

I convey my candid thanks to **Dr. Sanjay Sharma (Head of ECED), Dr. Amit Kumar Kohli (P.G. Coordinator),** and entire faculty of Electronics and Communication Engineering Department for their encouragement and cooperation.

Lastly, I would like to thank my parents and friends for their support and encouragement throughout making this report. They have always wanted the best for me and I admire their love and sacrifice.

Ambika Chhabra

801461003

ABSTRACT

Microstrip filters are the essential components for the microwave and millimeter wave applications like these are used in satellite, radar and mobile applications. The conventional filters are being replaced now days by a low loss and the miniaturized filters. Also, there is an increasing interest towards the EBG (Electromagnetic bandgap) structures. As they are capable to reject undesired frequencies therefore certain bandgaps are observed which can be used to make filters.

This thesis deals with the filters employing Electromagnetic bandgap structures. The first part deals with the technique to produce large attenuation in the stopband. A DMS (Defected Microstrip Structure) has been employed which causes large attenuation in the stopband. The structure with no DMS causes -20 dB attenuation and the structure with two DMS causes -25 dB attenuation whereas the structure with four DMS causes -30bdB attenuation in the stop-band. The second part deals with the tapering technique which minimizes ripples in the passband. In comparison to the Dolph - Tschebysheff array design, the Dolph - Tschebyscheff array design causes minor lobes with equal level but the Taylor produces inner minor lobe with constant amplitude and remaining minor lobes decrease continuously. The taylor tapering causes smoothening of the passband and produces large side lobe level on comparison with the uniform structure. The third part deals with a bandpass filter for S-Band applications which cover the frequency range from 2-4 GHz.

TABLE OF CONTENTS

CONTENTS **PAGE NO.**

CERTIFICATE AND DECLARATION i

ACKNOWLEDGEMENT ii

ABSTRACT iii

TABLE OF CONTENTS iv

ABBREVIATIONS vii

LIST OF FIGURES ix

LIST OF TABLES xii

CHAPTER 1. Introduction

1.1 Electromagnetic Band gap Structures 1

1.1.1 History 2

1.1.2 Principle of Electromagnetic Band Gap (EBG) structure 2

1.1.3 Surface Waves formation and method of reduction 3

1.1.4 Types of EBG 4

1.1.5 Difference between EBG and DGS 5

1.1.6 Improvements achieved by EBG 6

1.1.7 Application of EBG Structures in Microwave engineering 6

1.2 Microstrip filters 7

1.2.1 Design Considerations 7

1.2.2 Filter Characteristics 7

1.2.3 Filter Parameters 7

1.2.4 Filter Classification 9

1.2.5 Filter implementation 10

1.2.6 Scattering Parameters 11

1.2.7 Applications of EBG Filters 13

1.3 Gaps 14

1.4 Objective of Thesis 14

1.5 Thesis Organisation and Contribution 14

CHAPTER 2. Literature Survey

2.1 Introduction 16
2.2 Literature Survey 16
2.3 Conclusion 22

CHAPTER 3. A Miniaturized DMS Based Bandstop filter With large attenuation

3.1 Introduction 23
3.2 Filter Design 23
3.3 Microstrip Discontinuities 24
3.3.1 Microstrip Step and its equivalent circuit 25
3.3.2 Microstrip Gap and its equivalent circuit 26
3.4 Simulated Results and Discussion 28
3.5 Conclusion 29

CHAPTER 4. Dual Taylor Tapered microstrip filter Structure employing Electromagnetic Bandgap

4.1 Introduction 30
4.2 Filter Design 30
4.3 Tapering Technique 32
4.4 Comparison of Uniform EBG with the proposed Structure 33
4.5 Conclusion 36

CHAPTER 5. A Bandpass filter for S-Band Applications

5.1 Introduction 37
5.2 Filter Design 37
5.2.1 Design of High Pass filter 38
5.2.2 Design of Low Pass Filter 41
5.2.3 Cascading of High Pass and Low Pass filter 44
5.3 Simulated Results 44
5.4 Effect of dumbbell slots on the ground plane 45
5.5 Fabricated Band Pass filter and measured results 47
5.6 Conclusion 49

CHAPTER 6. Conclusion and Future Scope

6.1 Conclusion 50
6.2 Future Scope 50

References 51

List of Publications 55

Certificate of best paper award 56

ABBREVIATIONS

EBG	Electromagnetic Band Gap
DGS	Defected Ground Structure
RL	Return Loss
IL	Insertion Loss
VSWR	Voltage Standing Wave Ratio
SSN	Simultaneous Switching Noise
DMS	Defected Microstrip Structure
CST	Computer Simulation Technology
BPF	Bandpass Filter
SIW	Substrate Integrated Waveguide
LTCC	Low temperature co-fired ceramic
KFEBG	Koch Fractal EBG
RCS	Radar Cross section
PEC	Perfect Electric Conductor
BSF	Band Stop Filter
PBG	Photonic Band Gap
VSIEBG	Vertical Stepped Impedance
FCC	Federal Communications Commission
UCEBG	Uniplaner compact EBG

DAUEBG	Dual U-Shaped EBG
ELVEBG	Edge-located vias Mushroom type EBG
PIFA	Planer inverted F antenna
SAR	Surface Absorption Rate
CSRR	Complementary Split Ring Resonator
UWB	Ultra Wide Band
FDTD	Finite Difference Time Domain
CPW	Co-Planer Waveguide
SLL	Side Lobe Level
S-Band	Satellite Band
VNA	Vector Network Analyzer

LIST OF FIGURES

Fig. 1.1	2-D Mushroom type EBG	3
Fig. 1.2	Propagation of surface waves in substrate of patch antenna	4
Fig. 1.3	Blocking of Surface Wave by EBG structure	4
Fig. 1.4	Two dimensional planer Structures	5
Fig. 1.5	Three dimensional volumetric type	5
Fig. 1.6	The characteristic diagram of a general Filter	7
Fig. 1.7	Frequency band description	10
Fig. 1.8	Implementation of Richard's transformation	11
Fig. 1.9	Kuroda identities	11
Fig. 1.10	Two port network	13
Fig. 3.1	T-Shaped DMS	24
Fig. 3.2	Equivalent circuit of DMS	24
Fig. 3.3	Microstrip Step	25
Fig. 3.4	Equivalent circuit of Microstrip Step	25
Fig. 3.5	Microstrip Gap	26
Fig. 3.6	Equivalent circuit of Micrstrip Gap	26
Fig. 3.7	EBG structure with no hole	27
Fig. 3.8	A simple Bandstop filter	27
Fig. 3.9	A Bandstop filter with two DMS	27
Fig. 3.10	A Bandstop filter with four DMS	27

Fig. 3.11	S parameters for no hole EBG.	28
Fig. 3.12	S parameters of a simple Band stop Filter	28
Fig. 3.13	S parameters of a Bandstop filter with two DMS	28
Fig. 3.14	S parameters of a Bandstop filter with four DMS	28
Fig. 4.1	Array of Patches etched on Microstrip line	31
Fig. 4.2	3-D view of EBG Structure	31
Fig. 4.3	Taylor tapered Array of Patches and holes	32
Fig. 4.4	Simulated S_{11} parameters of 2-D uniform EBG microstrip structure	33
Fig. 4.5	Simulated S_{11} parameters of 2-D Taylor Tapered EBG Microstrip structure	34
Fig. 4.6	Simulated S_{21} parameters of 2-D uniform EBG Microstrip structures	34
Fig. 4.7	Magnified S_{21} parameters of 2-D uniform EBG Microstrip structures	35
Fig. 4.8	Simulated S_{21} parameters of Taylor Tapered EBG Microstrip structures	35
Fig. 4.9	Magnified S_{21} parameters of Taylor Tapered EBG Microstrip structures	35
Fig. 5.1	Bandpass filter	37
Fig. 5.2	Upper plane of a high pass filter	39
Fig. 5.3	Ground plane of a high pass filter	39
Fig. 5.4	Layouts of HPF	40
Fig. 5.5	Circuit Diagram of a HPF	40
Fig. 5.6	Complete layout of cascaded highpass filter	41
Fig. 5.7	Circuit diagram of Cascaded HPF	41
Fig. 5.8	Stepped impedance low pass filter with plane ground plane	42
Fig. 5.9	Circuit Diagram of a Low pass 7^{th} order filter	42
Fig. 5.10	Chebyshev coefficients for 0.1 dB ripple level	43
Fig. 5.11	Stepped impedance low pass filter with dumbell slots in the ground plane	43

Fig. 5.12	A Bandpass Filter without dumbell slots	44
Fig. 5.13	A Complete Bandpass Filter	44
Fig. 5.14	S21 of a High pass filter	45
Fig. 5.15	Simulated results of a low pass filter with planer Ground plane	45
Fig. 5.16	Simulated Results of a low pass filter with dumbell slots etched on the Ground plane	46
Fig. 5.17	Simulated results of a bandpass filter without dumbell slots	46
Fig. 5.18	Simulated Results of a complete bandpass filter	47
Fig. 5.19	Top view of a fabricated Bandpass filter for S-Band applications	47
Fig. 5.20	Bottom view of a fabricated Bandpass filter for S-Band applications	48
Fig. 5.21	Measured Results of a fabricated filter structure	48
Fig. 5.22	Filter testing on VNA	49

LIST OF TABLES

Table 1.1 Comparisons between EBG and DGS

Table 3.1 Specifications of DMS based Microstrip bandstop filter Structure

Table 4.1 Specifications of Taylor Tapered BSF

Table 4.2 SLL v/s B factor

Table 4.3 Comparison of Results of Uniform and Taylor Tapered EBG

Table 5.1 Specifications of proposed Bandpass filter

Chapter 1

Introduction

There is an elicit development in the UWB (Ultra wideband) systems, wireless internet for example WiFi (Wireless Fidelity) and WiMAX (Worldwide Interoperability for Microwave Access) Bluetooth due to which there is an increasing exuberance towards the microstrip filters. The filters basically protect one system from other by filtering out a wideband which is not required in UWB systems. The filters having sharper transition give more rejection for the signals which are out of band. The insertion loss is the amount of attenuation seen by signal through the pass band of the filter and is measured in dB. Any discontinuity in the microstrip line leads to additional inductance and capacitance and hence it is used to make filters. In microwave filters the challenges are to be faced in selectivity of the filters, bandwidth and miniaturization of filters. Because of the rapid development in the systems, it created more interest that enforces challenges on optimization, the various designs and understanding of components. To meet these challenges, there are so many techniques in which an EBG (Electromagnetic Band Gap) is the most common technique. Let us discuss EBG in brief.

1.1 Electromagnetic Band gap Structures

EBG are the most advance material in electromagnetic area. These are the periodic/aperiodic structures found in 1-D, 2-D or 3-D configuration. A multiple number of band gaps are observed which aren't only because of periodicity but the personal resonance of each element also. Due to interaction of microscopic (Mie) and macroscopic (Bragg) resonance, band gaps are formed. On co-incidence of two resonances, band gaps with maximum widths are observed. The main concentration is towards finding its tangible applications. Besides the great potential of EBG's, there is an abundance of applications in which they are used. EBG showcase a breakthrough w.r.t the planer methods. In order to take complete access to this technology, a transmitter or receiver internal components should be developed by using EBG. The method of finding electromagnetic band gap is from the dispersion diagram. For example, 0^0 reflection phase in the dispersion diagram represents the perfect magnetic conductor, where as 180^0 reflection phase in the dispersion diagram represents the perfect electric conductor. The

resonant frequency of a fixed wave number can be calculated from the Eigen mode solver this in turn used to describe the periodic properties of EM waves.

1.1.1 History

The electromagnetic band gap structure phenomenon appeared in 1960 in optical field. This phenomenon is based on the Total internal reflection. EBG's are generally a kind of Photonic crystals which can restrain the light completely [1].

In 1987, the two authors Sajeev John and Eli Yablonovitch put their great hands in describing the phenomenon of EBG structure [2] [3]. In 1980's Yoblonovitch said that at the various frequency bands, the periodic variation of refractive index is responsible of eliminating the spontaneous emission of photons. This has greatly affected the performance of many semiconductor devices like BJT's, FET's. Yablonovitch stated that a band gap can restrain the radiation of light induced, whereas John stated that a band gap can reflect on light waves to the focus. They had used the idea of Bragg reflection condition that is if the period is approximately $\frac{\lambda_g}{2}$, the EM wave will propagate in certain desired direction [2].

The first definition was provided by Shank and Kogelnik in the description of dispersion properties of distributed feedback lasers [3]. They didn't give the significance to the band gap feature caused by the periodicity of refractive index at that time. They proved that phenomenon through the equations of coupled waves. And, they figure it out by the help of Bloch-wave expansion method [4] and Couple Mode Theory through dispersion relation that due to the evanescent waves, there is a certain frequency band in which no propagation of EM wave takes place.

1.1.2 Principle of Electromagnetic Band Gap (EBG) structure

A standard EBG that is Mushroom type EBG is shown in the figure 1.1 in which the area of high impedance state shows range of frequency. The equivalent LC model which behaves as a filter to block the flow of surface waves in this frequency range. The current flowing through via holes can be represented by Inductor and the gap between adjacent patches is represented by the Capacitance. Hence, the increment in the inductance or the capacitance will automatically leads in the change of location of band-gap and will automatically leads to change in bandwidth and the other parameters also. The following

diagram shows the Mushroom type EBG and its equivalent L-C circuit and the formula to calculate cut off frequency, inductance, capacitance and bandwidth is shown [8]:

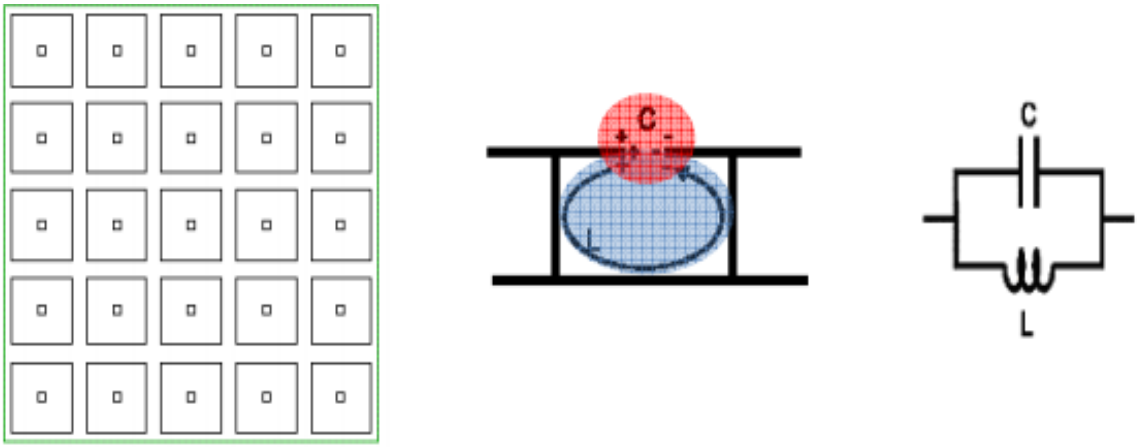

Fig. 1.1 2-D Mushroom type EBG [8]

The formula for calculating band gap central frequency is shown in the equation 1.1

$$f_c = \frac{1}{2\pi\sqrt{LC}} \tag{1.1}$$

$$L = \mu_o h \tag{1.2}$$

$$C = W\varepsilon_o \frac{(\varepsilon_r+1)}{\pi} cosh^{-1}\left(\frac{2W+g}{g}\right) \tag{1.3}$$

The bandwidth of the EBG is as follows:

$$BW = \frac{1}{\eta}\sqrt{\frac{L}{C}} \tag{1.4}$$

h: height of substrate

w: width of patch

g: distance of gap

1.1.3 Surface Waves formation and method for reduction

These are the waves which travel amidst two mediums of dissimilar refractive indices. In EMT or in Microstrip antennas, they travel in interior of substrate and remain or enclosed inside it until and unless it is met by any discontinuity. It is a kind of restricted EM

energy that acts like a standing wave. At the discontinuity, they create end fire radiation and produce comprehensive bandwidth. These can arouse when ε_r > 1. They can also leads to mutual coupling between the adjacent elements of an array. The proportion of power restricted inside substrate to that flowing in air is about$\left(\varepsilon^{\frac{3}{2}} : 1\right)^5$.

This law is in accordance with the principal of Total internal reflection (TIR) that if a wave is impinging at an angle more than $\left(\theta_c = sin^{-1}(\varepsilon^{-0.5})\right)$ critical angle, it gets TIR. These can be curtailed with the help of technique involving piles of substrate or cavities. But the main disadvantage of this technique is the increasing complexity and weight. Therefore, another alternative solution is the use of EBG [5]. Fig. 1.2 shows the propagation of surface wave in the substrate of patch antenna whereas the Fig. 1.3 shows the blocking of surface wave by EBG Structure.

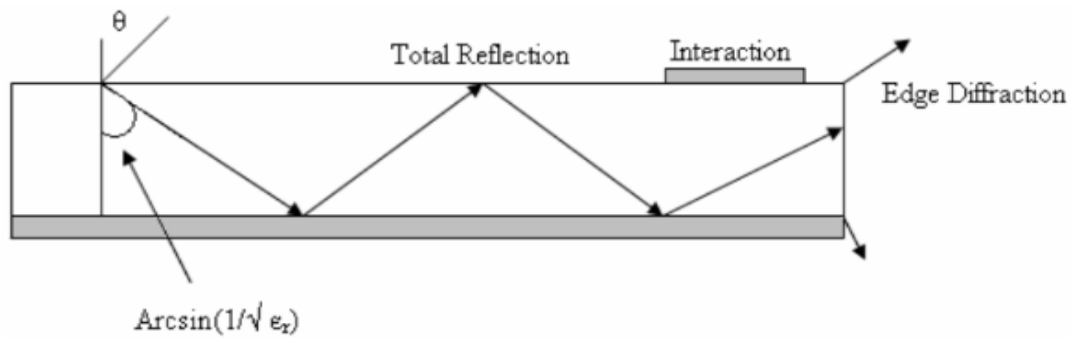

Fig. 1.2 Propagation of surface waves in substrate of patch antenna [6]

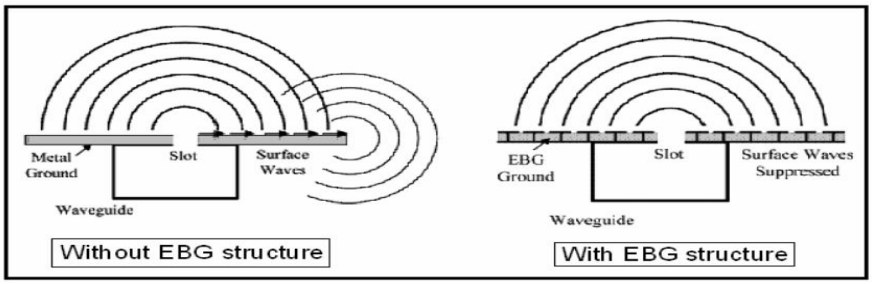

Fig. 1.3 Blocking of Surface Wave by EBG structure [7]

1.1.4 Types of EBG

According to the geometry, the EBG Structures can be categorized into three groups [8]:

(1) One dimensional Transmission lines

(2) Two dimensional planer Structures

(3) Three dimensional volumetric structures

Uni-planer Mushroom like

Fig. 1.4 Two dimensional planer Structures [8]

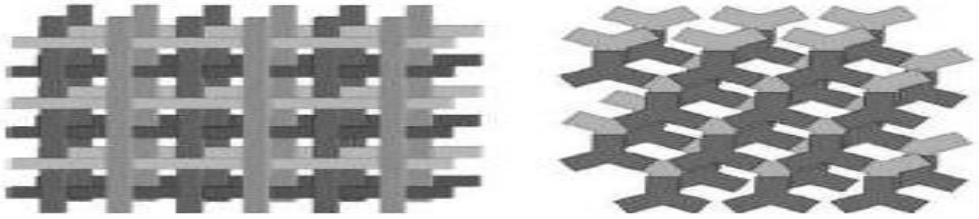

Woodpile dielectric Multilayer metallic tripod

Fig. 1.5 Three dimensional volumetric type [8]

Initially, the three dimensional EBG's were designed. These kinds of structures are having complete gap in bands. But the difficulty is in their fabrication. Hence two dimensional EBG's are more capable for fabrication process and exhibit similar properties and are more compact and stable as that of the 3-D EBG.

In 2-D EBG, propagation is along one axis and other parameters are constant along the third direction whereas in 1-D EBG, the index is only in one direction.

1.1.5 Difference between EBG and DGS

Table 1.1 describes the difference between DGS (Defected Ground Structure) and EBG structure.

The characteristics exhibited by of the DGS are:

- Has one-pole Low Pass Filter characteristics.

- Effects shielding fields on the ground plane.

- Reduces size for the component.

- Increases overall inductance and capacitance of the transmission line.

- Increases effective permittivity.

Table 1.1 Comparisons between EBG and DGS

Comparison	EBG	DGS
Geometry	Continuous etched structure (circles, squares etc.)	1 or 2 etched structures
Circuit extraction	Difficult	Simpler
Properties	Almost Similar	Almost Similar

1.1.6 Improvements achieved by EBG

1. Suppression of surface waves with the help of EBG provides an advantage in terms of battery duration enhancement.
2. Gain and axial ratio can be improved.
3. Provide high isolation and high quality factor.
4. Reflection phase characteristics for the low profile antennas.
5. Used for reducing circuit size.
6. Used for Mutual Coupling Reduction between adjacent antennas.
7. SLL of patch antenna can be improved.

1.1.7 Applications of EBG Structures in Microwave Engineering

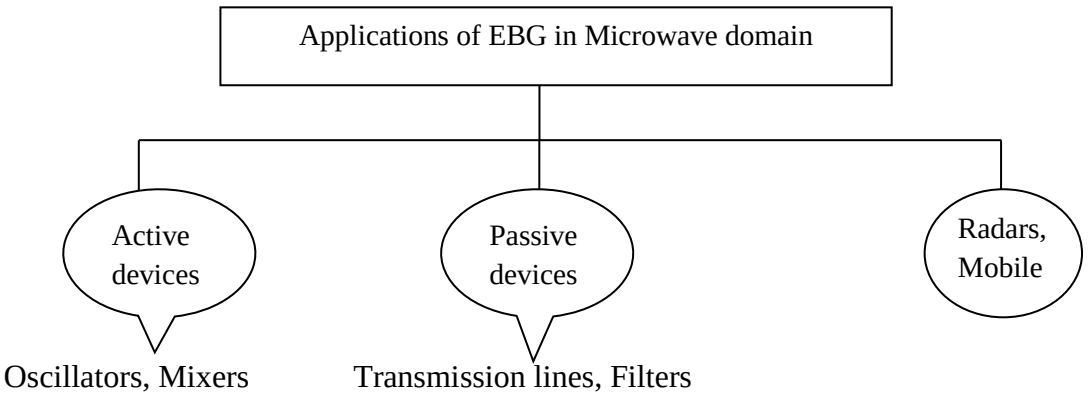

1.2 Microstrip Filters

Filters are used to confine Microwave or RF signals within the spectrum band by making low loss transmission in the passband while deep attenuation in the stopband.

1.2.1 Design Considerations:

The choice of geometry depends on the:

- Characteristic of filters like elliptic response or the Chebyshev response.
- Bandwidth
- Size
- RL (Return loss)
- IL (Insertion loss)
- Attenuation in the Stop-band
- Power handling capability

1.2.2 Filter Characteristics and its parameters

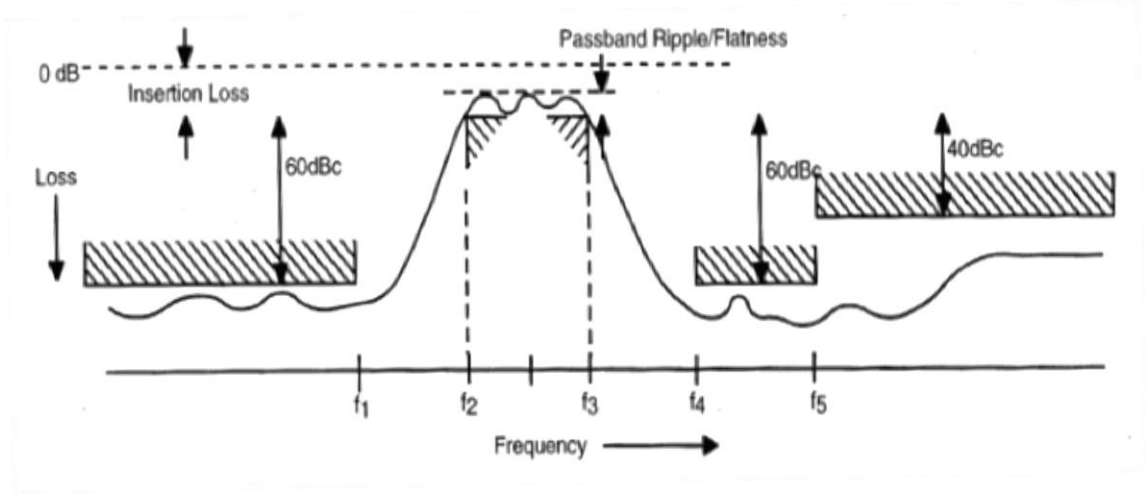

Fig. 1.6 The characteristic diagram of a general Filter

1.2.3 Filter Parameters:

- **Return loss (S11):** It is the loss in the signal power that occurs due to discontinuity problem in the transmission line. The power is reflected back to the same port. S11 = 0 dB means all the power is reflected, nothing is transmitted i.e.

that much band of frequency is not going to be radiated. It is expressed in decibels. The return loss is formulated as-

$$RL = -20 \log10 \left(\frac{Pi}{Pr}\right) \quad (1.5)$$

Where

Pi: Incident power

Pr: Reflected power

The source of loss is the reflection or the scattering. Higher return loss implies the better impedance matching and we are closer to the desired impedance. The another formula for calculating the Return loss is given as-

$$RL = 20 \log10 \frac{VSWR - 1}{VSWR + 1} \quad (1.6)$$

- **Insertion loss (S12):** It is the loss in the signal power which occurs due to the insertion of any device such as connector in the 50 ohm microstrip line. S21 = 0 dB means all the power is radiated, nothing is reflected back. Insertion loss is like Figure of Merit of the filter. For an extra loss, it is defined as positive where as if it is negative, then it is known as insertion gain. It is expressed in decibels. The insertion loss is formulated as-

$$IL = 20 \log10 \left(\frac{Pt}{Pr}\right) \quad (1.7)$$

Where

Pt: Transmitted power

Pr: Reflected power

- **Bandwidth:** It is a range of frequency or a band in which a signal can be transmitted without any kind of distortion or a range of useful frequencies around the resonance frequency. In other words bandwidth can also be defined as range of frequency in which a Return loss is maintained. Because the return loss tells the amount of power does an antenna accepts from the transmission line. In order to transfer the maximum power, the impedance of an antenna should be equal to the impedance of the transmission line. But the impedance of an antenna depends upon the frequency also. Because the impedance bandwidth depends on many parameters, therefore it is difficult to make calculations from a desired bandwidth point of view.

- **Power handling capability:** It is defined as the maximum power that a device can tolerate without being damaged. It is limited by the voltage breakdown and is directly proportional to the square of the voltage. The power handling capability should be as large as possible. It can be determined from the temperature rise of the conductor. The following parameters helps in determining the power handling capability:

  1. Thermal conductivity of substrate
  2. Ambient temperature (Ta)
  3. Transmission line losses
  4. Surface area of the conductor

  The thick substrates and the low impedance lines have higher power handling capability because the thick substrates for the same breakdown voltage can support higher voltages.

- **Attenuation in the stop band:** Depending on the application, the attenuation level should be in between 20 dB to 120 dB higher than the pass band attenuation level. The more is the attenuation the more selective is the filter, the more is the sharp roll off. The large attenuation in the stop band makes the filter to behave like an ideal filter.

- **Transition**: The other name of transition band is 'skirt'. It is defined as a range of frequencies that allows the transition between passband and the stopband. It is defined by the corner frequency or the cut off frequency. There should be a smooth fall off or the sharp transition in order to avoid problems.

- **Size:** The size should be as small as possible. Miniaturization of the filter size will leads to the reduction of overall cost as well as weight.

1.2.4 Filter Classification

The filter can be classified according to the domain in which it is used. Therefore the filter can be described as follows:

- Broadband/Narrowband (Frequency Band)

- Waveguide/Lumped
- Elliptic/Flat/Chebyshev (Topology)
- High pass/Low pass (Frequency Selection)

- **Filter Classification By Frequency Bands:**

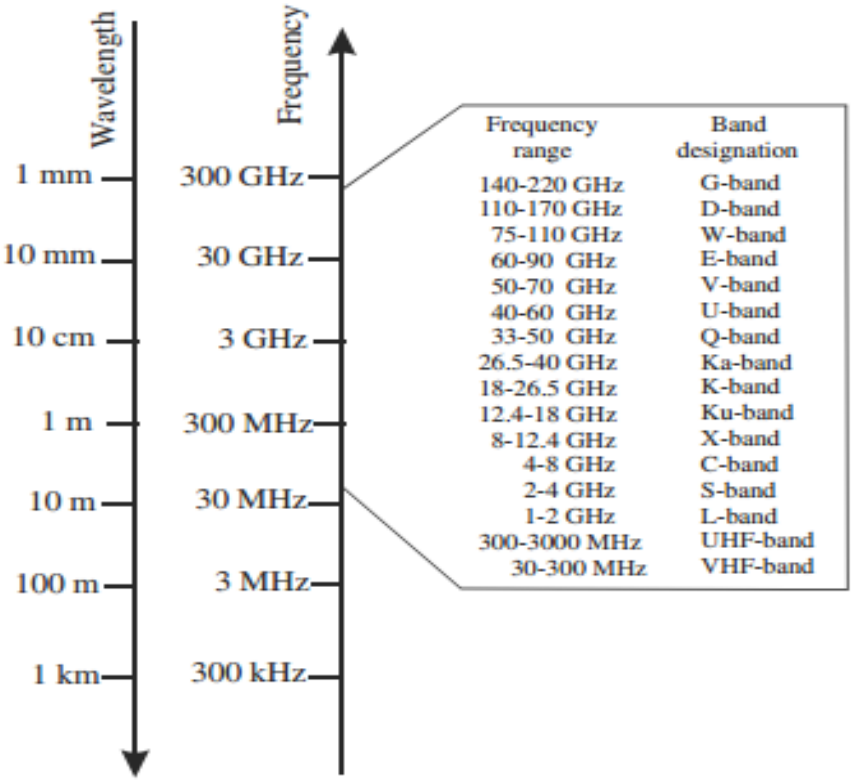

Fig. 1.7 Frequency band description [9]

1.2.5 Filter implementation

It's necessary to transform lumped elements into a microstrip filter therefore the Richard's transformation is used to do so. The Richards transformation is used to design Low pass filters. The reactance can be formulated as:

$$j * X_l = j\ L \tan \beta l \tag{1.8}$$

The susceptance can be formulated as:

$$j * X_c = j\ C \tan \beta l \tag{1.9}$$

Then the inductance and the capacitance can be replaced by their own impedance stub having length βl.

By making frequency is equal to one,

$$\tan(\beta l) = 1 \text{ implies } \beta l = \frac{\lambda}{8} \tag{1.10}$$

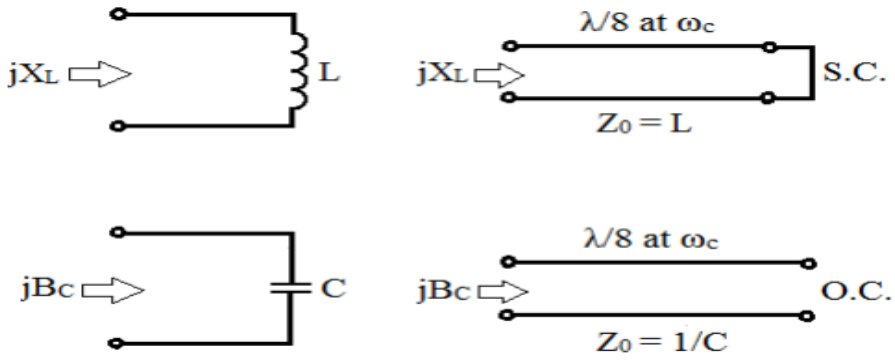

Fig. 1.8 Implementation of Richard's transformation [10]

Whereas the Kuroda's identity is used to convert shunt into series stubs or the series into shunt. For example,

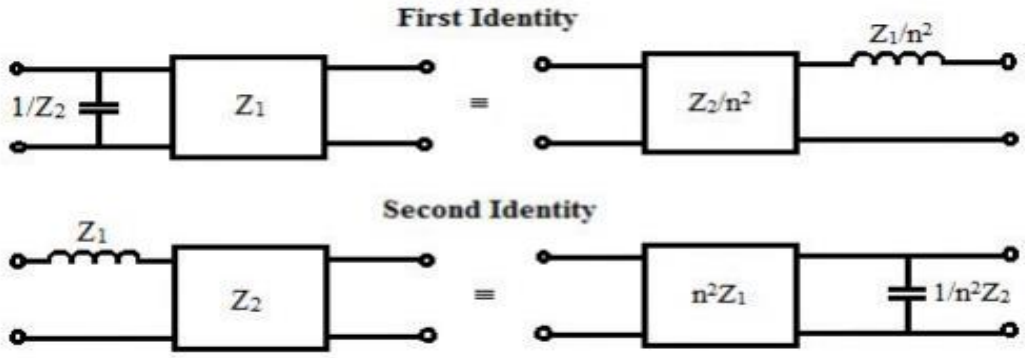

Fig. 1.9 Kuroda identities [10]

Where $$n^2 = 1 + \left(\frac{Z2}{Z1}\right) \tag{1.11}$$

1.2.6 Scattering Parameters

Depending upon the impedance, admittance etc. the range of frequencies are classified. Therefore, the S-parameters embody the effect of reflection or through transmission of power for any network. Whether the network is active/passive, two port/hundred port, the S parameters are very useful.

S-Parameters of a two-port network

The following two port network is terminated with the load resistance (Z_L) and having source resistance (Z_S).

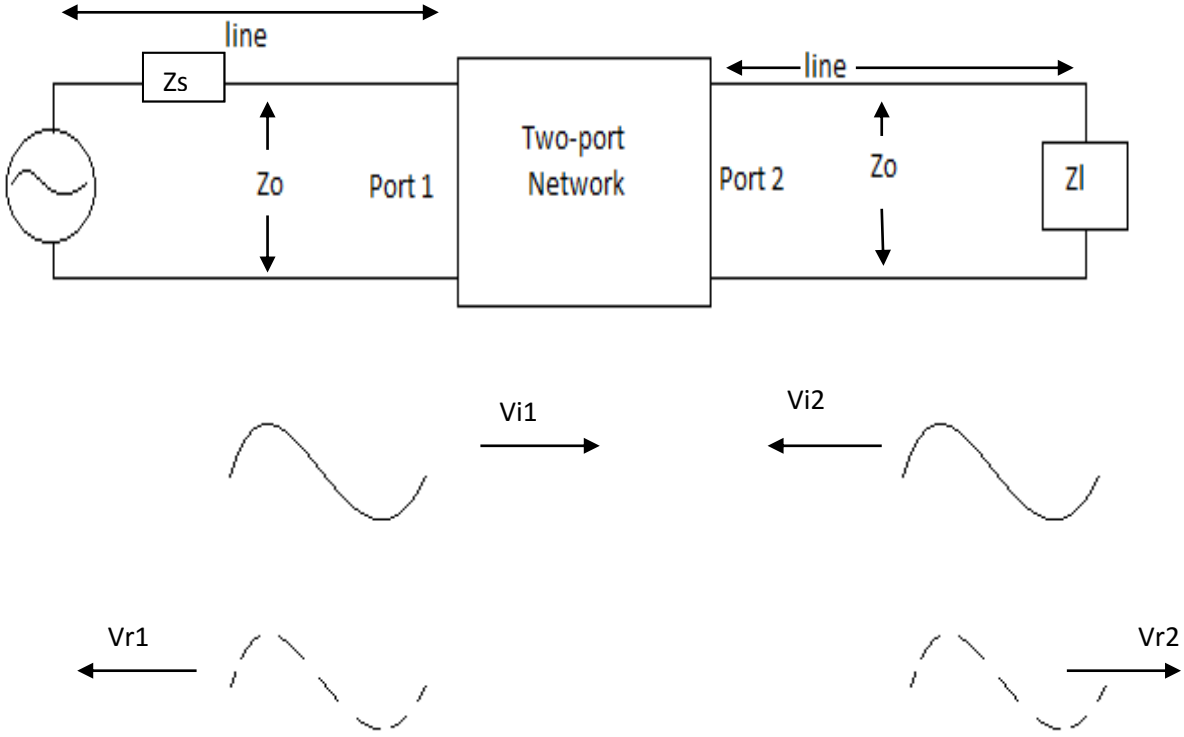

$$V_{r1} = x_{11}\ V_{i1} + x_{12}\ V_{i2} \quad (1.12)$$

$$V_{r2} = x_{21}\ V_{i1} + x_{22}\ V_{i2} \quad (1.13)$$

where

V_{in} is the incident voltage travelling towards the port n

V_{rn} is the reflected voltage travelling away from the port n

$$P_{i1} = \frac{|V_{i1}^2|}{Z_0} \quad (1.14)$$

$$a_1 = \frac{V_{i1}}{\sqrt{z_0}} \qquad b_1 = \frac{V_{r1}}{\sqrt{z_0}} \qquad a_2 = \frac{V_{i2}}{\sqrt{z_0}} \qquad b_2 = \frac{V_{r2}}{\sqrt{z_0}}$$

Therefore,

$$b_1 = S_{11}\ a_1\ + S_{12}\ a_2 \quad (1.15)$$

$$b_2 = S_{21}\ a_1\ + S_{22}\ a_2 \quad (1.16)$$

S parameter definition -

S_{11}: If $z_l = z_0$, therefore no reflections will take place at the load, $a_2 = 0$, Hence

$$S_{11} \xrightarrow{a_2 \to 0} \frac{b_1}{a_1} \tag{1.17}$$

Similarly, other three parameters can be defined as-

$$S_{22} \xrightarrow{a_1 \to 0} \frac{b_2}{a_2} \tag{1.18}$$

$$S_{21} \xrightarrow{a_2 \to 0} \frac{b_2}{a_1} \tag{1.19}$$

$$S_{12} \xrightarrow{a_1 \to 0} \frac{b_1}{a_2} \tag{1.20}$$

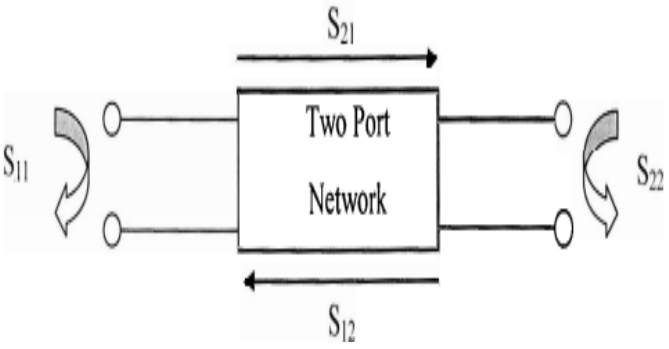

Fig. 1.10 Two port network

S_{12} is known as insertion loss which is a measure of attenuation where as S_{11} is known as return loss which is a measure of matching.

1.2.7 Applications of EBG Filters

1. Mobile for SSN Suppression. [11]

2. In Radar applications. [12]

3. Base Stations Receive Protection.

4. Base Stations Transmitters Filters.

6. Satellite Mobile Applications. [13]

7. EBG for duplexer networks.

1.3 Gaps

The below illustrated gaps are found in the previous literature:

- Small attenuation in the stopband.
- Large ripples in the passband.
- Poor selectivity.
- Low Optimized Bandwidth.

1.4 Objective of Thesis

Based on the gaps identified the following objectives are defined

1. Design and simulation of a DMS (Defected Microstrip Structure) based microstrip band stop filter with large attenuation in stop band.
2. Design and simulation of dual Taylor tapered microstrip band stop filter employing electromagnetic band gap structure with improved passband performance.
3. Design, simulation, fabrication and testing of a Microstrip band pass filter for S - Band applications.

1.5 Thesis organization and Contribution

The synopsis of the thesis is organized as following:

Chapter 1: The knowledge of EBG and principal behind that, the improvements achieved by EBG and its applications and the contribution of microstrip filters has been discussed. Also, how the microstrip bends and gaps leads to effective inductance and Capacitance and the formulation of S-Parameters has been briefly described. The equivalent circuit and the designed formulas of calculating the inductance and capacitance of Microstrip bends and gaps are shown in this chapter.

Chapter 2: A concise literature review on the Microstrip filters employing electromagnetic band gap. Various methods have been adopted to improve filter response i.e the insertion loss, the return loss, the stop band attenuation, the bandwidth and the method to curtail the ripples caused due to the periodicity of the structure has been described in this chapter

Chapter 3: investigates the miniaturized DMS based Microstrip band stop filter. The design and simulation was done with the help of CST Microwave studio 2014. The technique of improving bandwidth and increasing attenuation has been described in this chapter. The simulation results have also been bestowed in this chapter.

In this, the bandwidth is enhanced by etching circular hole in the ground plane whereas the large attenuation is achieved by making defects in the microstrip line itself.

Chapter 4: The design and simulation of Taylor Tapered bandstop filter employing Electromagnetic bandgap. Tapering is done to eliminate ripples in the passband. In this structure, Taylor distribution of uniform array is adopted. Comparison of Side lobe level and ripples in the pass band between Uniform and Taylor tapered EBG structure has been shown. A smooth passband and a higher Side lobe level have been obtained by using the Taylor tapering distribution on comparison with uniform or the other tapering techniques. Complete description of the technique and the formulas associated for finding the tapering coefficients or the weight factors has been given in this chapter.

Chapter 5: The design, simulation and the fabrication of Microstrip bandpass filter for S-Band (Satellite Band) applications. The whole structure is substituted into different parts and the separate analysis and simulation is done for each substituent section. The bandwidth of 2-4 GHz has been observed after simulation which can be used for the S-Band applications. Also, the fabricated structure of the proposed filter has been added along with the tested results in this chapter and it has been observed that the measured results are in good agreement with the simulated results.

Chapter 6: In this chapter, the discussion about microstrip filter for wireless applications, the design procedure and fabrication for the microstrip filter has been discussed. The future scope does the microstrip filters contribute has been demonstrated.

Chapter 2

Literature Survey

2.1 Introduction

The first stage of designing an improved filter is to study the research papers that have been written previously by other researchers. The papers that are related to this title are chosen and studied. EBG structures of different shapes are used to suppress the surface wave, increase the directivity and gain and to reduce the back radiations. With the help of this literature review, it gives more clear understanding to perform this report.

2.2 Literature Survey

John D. Shumpert, *et al*. (1999) proposed the technique for the enhancement of bandwidth and the radiation pattern with the help of resonant slot on the reflecting plate and by filling the resulting plate with an artificial EBG. These also helped in eliminating radiation from the back side of the slot. Firstly a half wavelength slot was made but it caused difficulty in matching between the CPW (Co-planer waveguide) feed and the slot, therefore a full wavelength slot was made. The full wavelength slot not only improved matching but improved bandwidth also. The substrate used was thick in this paper, but if used as thin material similar results will be obtained. So, a little power was lost. Therefore, these kinds of filters require packaging when used in certain applications. [14]

Shau-Gang Mao, *et al*. (2001) proposed a one dimensional EBG for conductor backed CPW. In this EBG is made on both the microstrip and the upper ground plane. The equivalent circuit is also made. On cascading the EBG cells, the low pass filter with lower cut off frequency with a wide bandstop is observed. The proposed structure can be used in MMIC applications for example amplifiers, filters, antennas and mixers. In this the radiation losses also gets minimized. [15]

William J. Chappell, *et al.* (2001) designed a high Q factor filter without using any kind of tuning. The EBG was used to suppress the substrate noise. Because of the low loss property of resonators, a low insertion loss was observed. As the constant coupling coefficient filters generally exhibit low insertion loss, therefore by not changing the lattice parameters of the filter, a filter with fixed coupling coefficient was constructed.

The substrate used was Duroid. The filter was having the center frequency of 10.7 GHz. The fractional bandwidth of the filter was 2.7%. Also to provide the low insertion loss or to couple the filter, the length of the CPW feed was adjusted. The out of band isolation was restricted by the coupling of the CPW lines, therefore the space wave coupling of CPW lines was removed by packaging the CPW lines. [16]

Yasushi Horii, *et al*. (2002) proposed a method of controlling the harmonics in microstrip patch antenna. The substrate used was RT/Duroid 5870. The twelve slots were etched on the ground plane. For the broad bandwidth, a square patch was made above the substrate. The antenna was fabricated by LPKF F'rotoMat C30S (cutting machine). In this, the FDTD (Finite Difference Time Domain) Simulations were done and the second and the third harmonic were controlled. A bandwidth was widened from 2% to 14.7% with VSWR less than 2. The radiation pattern was calculated at 2.15 GHz, 2.30 GHz and 2.45 GHz and front to back ratio more than 16 dB was obtained. The axial ratio obtained was more than 30dB. [17]

Hsiuan-ju Hsu, *et al*. (2002) proposed an X-band three pole BPF based on the Chebyshev topology. This structure comprised of the three EBG cavities and was able to achieve at f_{res} of 9.72GHz, a 5.95 percent BW response and a large isolation. The spacing between metallic walls and coupling between adjacent slots was taken as less than $\lambda_g/2$ and L/4 respectively. At the center of coupling slot, a shorting via was used to make short circuit. HFSS was used to simulate the proposed structure. [18]

C.C. Chiau, *et al*. (2003) proposed a multi-period EBG structure using FDTD simulation for wide stopband circuits. In this single period EBG structures are cascaded. It was assumed that the stopband gets widened after cascading single period EBG structures together. The transmission characteristics of the proposed structure were also discussed. The circles were etched which on increasing will leads to deeper attenuation in the stop band. [19]

M.F. Karim, *et al*. (2004) presented a novel design of Hybrid EBG (H-EBG). A Keiser Tapering distribution was used to highly reject bandwidth. A C-band Low pass filter characteristics were observed. And a comparison was made between Hybrid-EBG and a stepped impedance EBG filter and it was shown that Hybrid-EBG had a magnified performance over the stepped impedance. The insertion loss was found out to be below 0.25 dB and the rejection bandwidth was above 12 GHz. [20]

Shao Ying Huang, *et al.* (2005) designed Band Stop Filter (BSF) comprises planer-modulated microstrip and holes are carved in the ground plane. In this, comparison is obtained in single plane tapered and double plane tapered structure and different Tapering Techniques were adopted like Hamming, Hanning, Blackmann, exponential, cosine, gaussian, Bartlett and their performance was compared. It was observed that in dual plane tapered structure, a Chebyshev Tapered EBG structure shows excellent Performance among different Tapering Techniques. And ripples in the passband in dual plane Tapered structure were less as compared to single plane Tapered structure but the stop band characteristics were poor. [21]

Shao Ying Huang, *et al.* (2005) designed a Low pass Filter (LPF) comprises of the U-Shaped Modulated-microstrip structure and carved holes on ground plane. Chebyshev Tapering of antenna array theory was adopted in order to reduce ripple level in the passband and have high attenuation magnitude in the stopband. The structure was able to obtain good passband and stopband performance as well. [22]

Joan Garcia-Garcia, *et al.* (2006) developed a new technique to form an UWB Bandpass filter. Instead of cascading High and Low pass filter to form a Bandpass which results in increasing size, a new technique of mixing high and low pass filter was formed. In this, a 2 stage Electromagnetic band gap structure comprises a Microstrip line loaded with shunt short circuited stubs and patches were made. And an UWB Bandpass filter with bandwidth of 4.8 GHz with center frequency of 3.4 GHz was designed. [23]

M. F. Abedin *et al.* (2008) proposed a new structure for large stop band for surface wave and also provide large attenuation in the stop-band. To calculate the frequency of the surface wave, a formula has been developed. The better results have been observed in the case of TMM and Duroid substrate. This structure also provides the feature of in phase reflection of the wave in 1.8 GHz range by making thin directional cylindrical dipole antenna. [24]

Jung-Woo Baik *et al.* (2008) proposed two band pass filters for size reduction with the help of UC-EBG and Foliated UC-EBG. The UC-EBG was split into the four sections and further each section was split into four sections in the FUC-EBG cell. The overall size was reduced to 22% and 24% respectively for both the filters. The size reduction was observed due to the quasi-static lumped element's slow wave effect. [25]

Dong-Jin Jung and Kai Chang, *et al.* (2009) mathematically analyzed the technique of integration of LPF with a dumbbell shape DGS. An equivalent circuit of DSS was made. Separate analysis and alteration of design equation according to the parasitic inductance of stub in LPF was done. The transmission line concepts were used in designing the equations of parasitic inductance of the stub. The measured insertion loss was found out to be less than -0.2 dB. [26]

Lin Peng, *et al.* (2010) made a Mushroom-like EBG integrated with CSRR (Complementary split ring resonator). On comparison with the conventional EBG, the proposed structure had shown a 28% miniaturization in size. Due to asymmetric structure, the band gap properties are different in both the X and Y direction which were found at 3.35 GHz to 5.10 GHz frequency. Also in the Y direction, two extra tunable bands were observed at 6.02 GHz to 6.65 GHz frequency. The location of band gaps could be easily checked from the Brillouin dispersion diagrams. The use of this type of EBG structure can be found in dual or the triple band applications. [27]

B.-W Liu, *et al*. (2011) designed an UWB-BPF consists of two mushroom-like EBG's producing two precise notches. The structure also consists of dual EBG closer to the feed which on having change in dimensions produce changes in the center frequencies. On changing the physical dimensions of the EBG Structures, the notch bands central frequencies became 5.2 GHz and 5.8 GHz. And also two Microstrip lines were coupled with ground plane open end co-planer waveguide. The two notches produce BPF behavior with bandwidth of 5.7 GHz. The advantage of this type of filter structure is the small size and good performance. [28]

Sang il Kwak, *et al*. (2011) proposed PIFA (Planer inverted F antenna) with EBG for SAR (Surface absorption rate reduction). An SAR causes several health problems. In this EBG was used to combat undesired radiations and the surface waves. Hence a human brain is prevented from the harmful EM radiations produced from Mobile. EBG works as a perfect magnetic conductor for improving the performance of an antenna. First, the integration of PIFA and an EBG cells was done. EBG was applied on the mobile's ground plane. Further, a parametric study on location of antenna, antenna height and the number of EBG cells was done. The measured RL was 1.84 GHz - 1.91 GHz with VSWR less than 3. Finally, the Surface absorption rate was reduced by 31% by using PIFA with EBG. [29]

Lin Peng, *et al*. (2012) proposed a multiple band gaps based EBG Structure named DAU-EBG (Dual U-Shaped) in which the U type slots were carved w.r.t axis on ELV-EBG (Edge-located vias Mushroom type). By adjusting slot parameters, resonant frequencies can be tuned. Because of an asymmetric structure of the U-type slots, the bandgaps in two orthogonal X and Y directions are observed. The three bandgaps in X direction and the two bandgaps in the Y direction were obtained. A size reduction of 74% and 62% was achieved as compared to the CMT-EBG and ELV-EBG. This structure can be used for the multi-band applications. [30]

Haoran Zhu, *et al.* (2012) added the new concept of patch loaded with stubs and the spurline to get high attenuation in the stop band and wider stop band. As both can introduce zeros in the stop band. Further the size of the filter was decreased by using the third order filter as the third order filter was giving better response than a fifth order filter. And the ripples caused on account of periodic nature of EBG were minimized by using Chebyshev distribution of antenna array. An UWB band-stop from 3.6 to 10 GHz was obtained, with achieved attenuation magnitude below -20 dB and a smooth passband was obtained. [31]

Chen Fei Su, *et al.* (2013) cascaded a High pass and a Low pass to form Band Pass Filter Structure. A separate analysis on both Filter structures and on cascading both structures was done. A Chebyshev technique was used on the etched patches in the ground plane and the patches on the Microstrip line to taper in order to eliminate ripples from the Passband. Changing the filling factor alters the cut-off frequency. The lumped element consists of three inductors and four capacitors. The simulated insertion loss was less than 1.5 dB with sharp transition from pass band to stop band. An Ultra-wide Bandpass with bandwidth from 3.1 GHz to 10.6 GHz was observed. [32]

Sridhar Raja, *et al*. (2013) in order to achieve FCC Limit, proposed an UWB (3.1 - 10.6 GHz) Band pass Filter. In this, the EBG structure was described with three different configurations viz. Uniplaner, Mushroom type and Fork like EBG structure respectively. The UC-EBG (Uniplaner compact) consists of coupled lines of interdigital type which is commonly used in the several BPF's. A good Passband and beside Passband (or out of band) performance with improved selectivity was obtained. The simulation was done by using ADS simulator. [33]

Myunghoi Kim, *et al.* (2013) proposed a VSIEBG (Vertical Stepped Impedance) EBG Structure formed by low and high impedance lines and vertical branch, for SSN (Simultaneous Switching Noise) Suppression. On using capacitors and hybrid EBG, an Ultra-wideband suppression is observed. An equivalent circuit of the same was made and it was observed that SSN suppression between 650 MHz - 20 GHz below -40dB along with 86% size miniaturization was obtained. And the lower cut off frequency was decreased to 650 MHz from 2.4 GHz. [34]

Zhaowen Yan, *et al.* (2014) designed an EBG structure with three layers. First a 2-D EBG was formed which comprises a power plane carved with 3 by 3 EBG cells and a plane ground plane. Then a three layer EBG structure wrapped with plane was formed which did not show a good SSN suppression as an EBG diminishes its action of noise filtering when placed in strip-line environment therefore the noise can be suppressed by adding vias. And the attenuation and stopband curve depends on the number of vias. Finally a stop-band between 1.10 GHz - 21.53 GHz with attenuation less than -30dB was obtained. [35]

Pooja Sahoo, *et al*. (2014) proposed a BSF (Band stop filter) consisting Open circuit stubs with f_c of 2.2 GHz and 1.7 GHz respectively. Comparison was made between the L type, optimum and a filter with a Chebyshev topology. Then filter was integrated with PBG. Results are compared by using T shape and an E shape PBG. The complete mathematical analysis was done to obtain the desired filter response. The proposed structure had a wide bandgap in the stopband and a comparison was made between filter with PBG and a filter without PBG. No change was observed in insertion loss but the slow wave factor gets increased on comparing the proposed structure with a conventional structure. On using photonic bandgap structures the sidebands gets minimized and bandwidth gets improved up to 30%. [36]

Constantine A. Balanis, *et al*. (2015) proposed a method for RCS (Radar cross-section reduction). In this, a comparison was made between a hexagonal checker board and a square checkerboard and measured. EBG dual planer structure provided the 63% reduction, Hexagonal structure reduced Radar cross-section lobes. The lobes appear because the surface of the checkerboard reflects energy instead of absorbing it. At the end, this technique was able to achieve Radar cross-section minimization up to 10dB on

comparison with PEC at the 60% frequency band of checkerboard and also was able to achieve mono static RCS pattern. [37]

Juan de Dios Ruiz, *et al*. (2015) formed a Koch-fractal type electromagnetic filter structure in single dimension. In this, the filling factor R/A is adjusted to be greater than 0.5 value but this leads to ripples in the pass band. Hence in order to combat or overcome this, several tapering functions are adopted. A is changed continuously to combat variation in R/A ratio. The new technique of scaling tapering coefficients by K was done. To this KF-EBG, Cauchy and Kaiser Windowing were applied. For double layer Tapering, Cauchy windowing was applied with K taken as 1.25 and to single side Kaiser Windowing was applied with K taken as 0.9. [38]

Juan de Dios Ruiz, *et al*. (2015) proposed a new technique of making Bandpass Filter which comprises of the HMSIW (half mode substrate integrated waveguide), the SIW (substrate integrated waveguide) integrated with an etched KF-EBG on the surface of waveguide. The filling factor was taken as greater than 0.5. The filter response was enhanced with the help of windowing technique to Koch Fractal shape. The insertion loss was found to be less than 1.7dB and the return loss was found to be greater than 11.4dB. The Stopband attenuation greater than 39dB was obtained. [39]

Sai Wai Wong, *et al.* (2015) proposed a BPF comprising SIW (substrate integrated Waveguide) using LTCC (Low temperature co-fired ceramic) Technology. The structure comprises of cascade of three EBG Structures i.e. SIW, metallic vias and U slots. The vias were used to restraint or limit the coupling but were unsuccessful to produce that much amount of coupling in order to obtain the desired bandwidth so U slots were carved on the SIW to obtain Band pass filter with bandwidth of 40GHz. According to the gap, height, width of the slot, Q (Quality factor) and K (Coupling coeff.) were formulated. [40]

2.3 Conclusion

From the literature survey, it has been concluded that many filter structures have been designed and discussed using EBG. But these structures are having some drawbacks such as large ripples in the passband, low attenuation in the stopband and a very low bandwidth etc. In this thesis we have tried to improve certain drawbacks in the above discussed research papers. The following chapters will describe the work which has been done to overcome the gaps and to curtail the drawbacks of the above research work.

Chapter 3

Miniaturized DMS based Microstrip band stop filter with large attenuation

3.1 Introduction

In recent years, there is an increasing interest to combine the microstrip structures and photonic band gap structures (PBG), defected ground structure (DGS). As similar to DGS, defected microstrip structure (DMS) also disturbs current distribution and exhibits band stop properties. Similar to DGS, the DMS has also been applied to improve performances of microwave circuits like harmonic termination networks in power amplifier, filters, antennas etc.

DGS defect in ground plane disturbs the shield current distribution and performs a band-gap behavior in some frequency band with only one or more unit patterns, and the DMS also changes the current distribution and leads to resonant circuit of inductance and capacitance.

The DMS has been used to improve isolation between the two ports in patch antenna and can also be used to achieve desirable coupling between the coupled microstrip lines for size reduction in power dividers. Moreover, DMS is employed with BPF to simultaneously produce band stop and band pass response and to curtail ripples in the pass band response.

The stepped impedance is used to design filters but the limitation of Stepped impedance filters is low attenuation and the low selectivity therefore, a DMS is used here. Unlike a spur line and an open stubs [21] used to combat the low attenuation and low selectivity, a combination of DGS and a T-shaped DMS structure with small size is proposed which is made by inserting imperfections or defects in the microstrip line, as slot in the microstrip line also causes resonant behavior in the frequency response.

3.2 Filter Design

The design comprises of modulated Stepped impedance Microstrip line with square patches whose area is taken as 5*5 mm^2 i.e. the length and width of the square patch are 5 mm and 5 mm respectively. The overall size of the structure is 35*20 mm^2. The substrate

is taken as FR-4 with dielectric constant and a thickness of 4.3 and 1.6 mm respectively. As the defects in the ground plane will leads to the change in resonant frequency therefore, in order to improve bandwidth, the circular holes are etched on ground plane with radii of 5 mm.

The DMS comprises of Horizontal and a vertical slot with the following dimensions listed as follows.

Table 3.1 Specifications of DMS based Microstrip bandstop filter Structure

Variables	**Specifications(in mm)**
La	4
Lb	0.5
Wa	0.5
Wb	0.5
L	5
Radii of slot in the ground plane	5
Copper thickness	0.035

The filling factor (length of patch/diameter of hole) is taken as 1. In this, the effective inductance can be altered by horizontal slot whereas the capacitance can be altered by the vertical slot. Therefore the resonant frequency can be changed by horizontal slot and the vertical slot also.

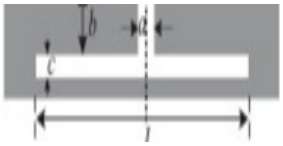

Fig. 3.1 T-Shaped DMS

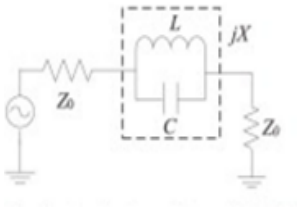

Fig. 3.2 Equivalent circuit of DMS

3.3 Microstrip Discontinuities

A discontinuity can be in the form of a gap, a step, open ends, right-angled bends, T-junction, cross-junction etc.

3.3.1 Microstrip Step and its equivalent Circuit [41]

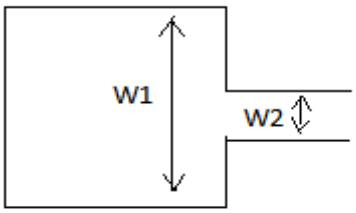

Fig. 3.3 Microstrip Step [41]

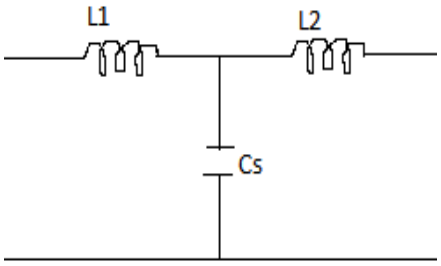

Fig. 3.4 Equivalent circuit of Microstrip Step [41]

$$L_{w1} = \frac{Z0 * \sqrt{\varepsilon_{re}}}{c} \quad (3.1)$$

$$L_{w2} = \frac{Z0 * \sqrt{\varepsilon_{re}}}{c} \quad (3.2)$$

The total Inductance L_t is divided into L_1 and L_2 using inductance division rule as:

$$L_1 = \frac{Lw1}{Lw1+Lw2} * L_t \quad (3.3)$$

$$L_2 = \frac{Lw2}{Lw1+Lw2} * L_t \quad (3.4)$$

L_t is given by:

$$L_t = h* \left[\left(-40.5 * \left(1 - \frac{W1}{W2}\right)\right) + \left(75 * \log\frac{W2}{W1}\right) + \left(0.2 * \left(1 - \frac{W1}{W2}\right)^2\right)\right] \quad (3.5)$$

Cs is given by:

$$Cs = \sqrt{W1 * W2} * \left[\left(\frac{W1}{W2} * \left(2.33 + (10.1 * \log\varepsilon_r)\right)\right) - 12.6 * \log\varepsilon_r - 3.17\right] \quad (3.6)$$

when $1.5 < \frac{W1}{W2} < 3.5$

$$\text{than } Cs = \sqrt{W1 * W2} * \left[130 * \log\left(\frac{W1}{W2}\right) - 44\right] \quad (3.7)$$

3.3.2 Microstrip Gap and its equivalent circuit

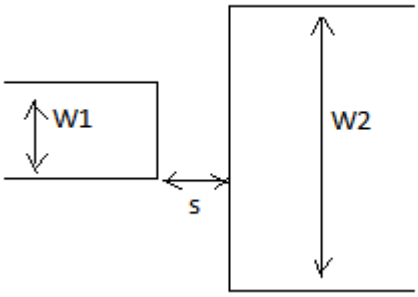

Fig. 3.5 Microstrip Gap [41]

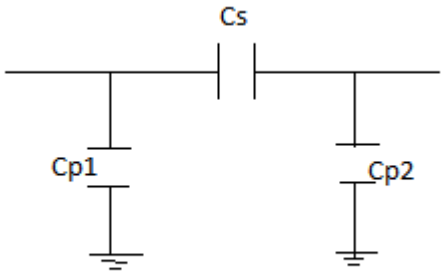

Fig. 3.6 Equivalent circuit of Micrstrip Gap [41]

$$C_s = 500*Q_1*h*\left(1+4.19*\left(1-exp\left(-0.785*\sqrt{\frac{h}{W1}}*\frac{W2}{W1}\right)\right)\right)*\exp\left(1.86*\frac{s}{h}\right) \quad (3.8)$$

$$Cp_1 = C_1 * \frac{Q2+Q3}{Q2+1} \quad (3.9)$$

$$Cp_2 = C_2 * \frac{Q2+Q4}{Q2+1} \quad (3.10)$$

Where

$$Q_1 = 0.04598*\left(0.03+\left(\frac{W1}{h}\right)^{Q5}\right)*(0.272+0.07*\varepsilon_r) \quad (3.11)$$

$$Q_2 = 0.107*\left(9+\left(\frac{W1}{h}\right)\right)*\left(\frac{s}{h}\right)^{3.23}+2.09*\left(\frac{s}{h}\right)^{1.05}*\frac{1.5+0.3\frac{W1}{h}}{1+0.6\frac{W1}{h}} \quad (3.12)$$

$$Q_3 = \exp\left(-0.5978*\left(\frac{W2}{W1}\right)^{1.35}\right)-0.55 \quad (3.13)$$

$$Q_4 = \exp\left(-0.5978*\left(\frac{W1}{W2}\right)^{1.35}\right)-0.55 \quad (3.14)$$

$$Q_5 = \frac{1.23}{1+0.12*\left(\left(\frac{W2}{W1}\right)-1\right)^{0.9}} \quad (3.15)$$

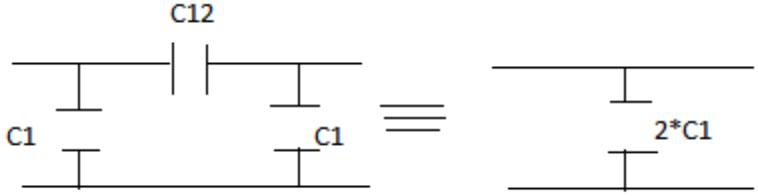

$$C_{even} = 2*C_1 \quad (3.16)$$

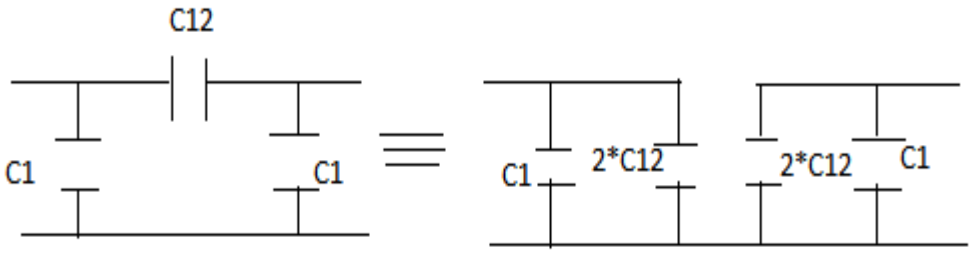

$$C_{odd} = 2*C_{12} + C_1 \quad (3.17)$$

C_{even} arises if the 2-port network is excited symmetrically and C_{odd} arises when 2-port network is arises asymmetrically.

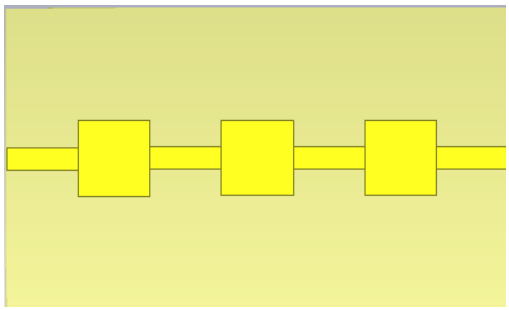

Fig. 3.7 EBG structure with no hole

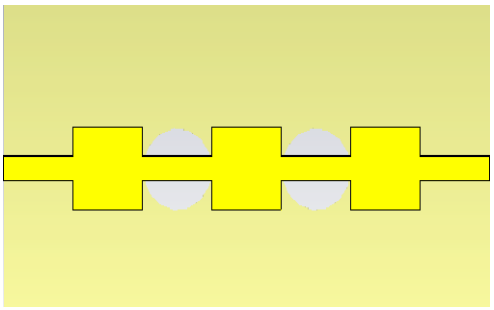

Fig. 3.8 A simple Bandstop filter

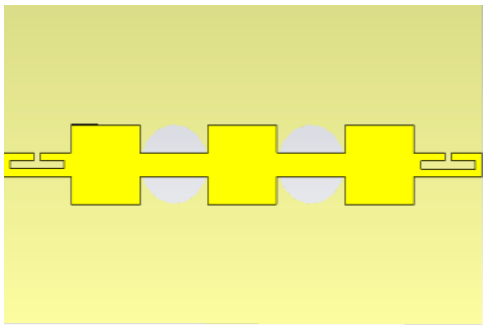

Fig. 3.9 A Bandstop filter with two DMS

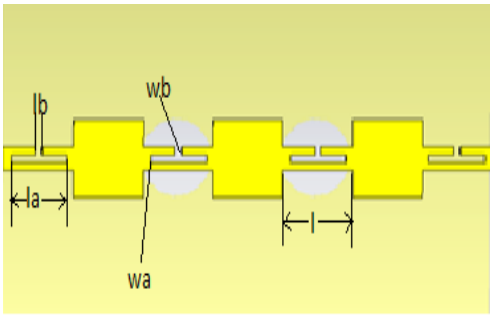

Fig. 3.10 A Bandstop filter with four DMS

Firstly, a simple bandstop filter with no hole and with two circular holes is simulated, and then a bandstop filter with DMS is simulated.

Fig. 3.1, Fig. 3.2 shows the T-shaped defected microstrip structure and its equivalent circuit respectively.

Fig. 3.7 and Fig. 3.8 shows the simple stepped impedance Bandstop filter with no hole and with two slots etched on the ground plane respectively.

Fig. 3.9 shows a Bandstop filter with two defected microstrip structures whereas Fig. 3.10 shows a Bandstop filter integrated with four DMS.

3.4 Simulated Results and Discussion

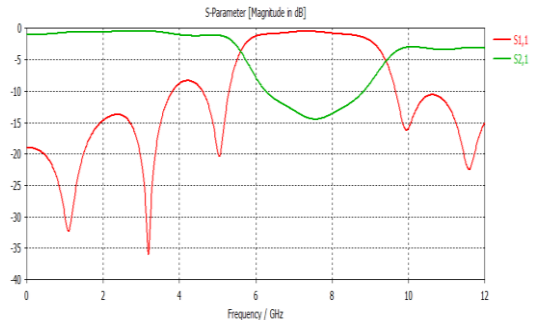

Fig. 3.11 S parameters for no hole EBG.

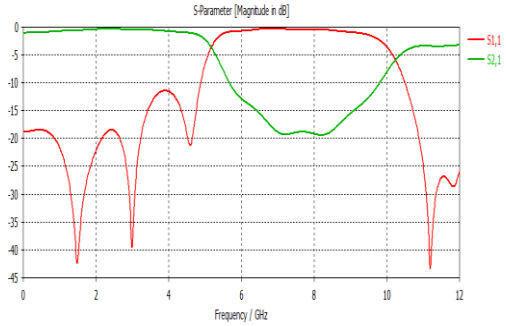

Fig. 3.12 S parameters of a simple Band stop Filter

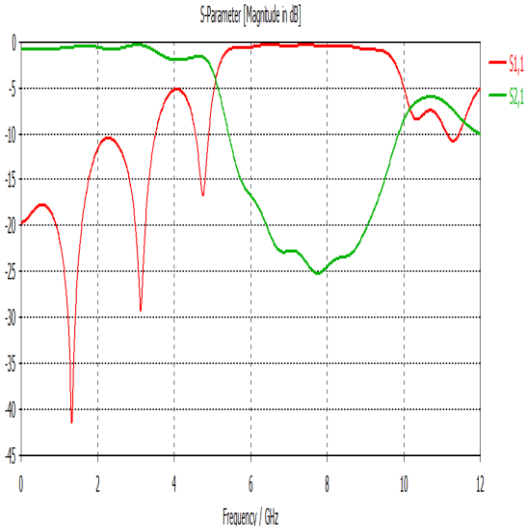

Fig. 3.13 S parameters of a Bandstop filter with two DMS

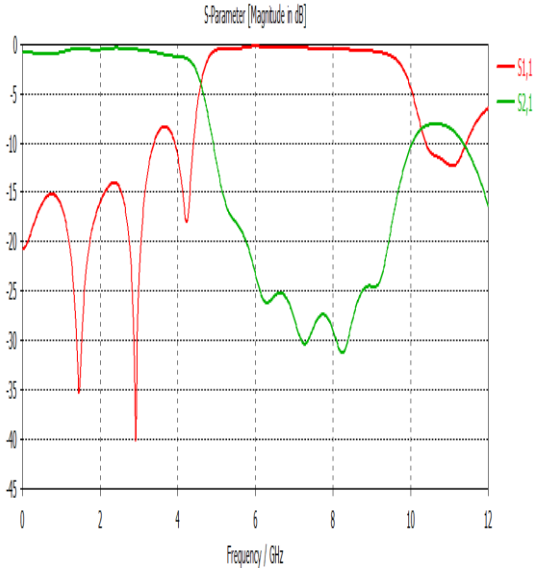

Fig. 3.14 S parameters of a Bandstop filter with four DMS

As it can be seen from Fig 3.11 that a simple Band stop filter with no hole has stop band from 6 Ghz to 9 Ghz with stop band attenuation of -15 dB.

Fig 3.12 shows that bandstop filter with defects on the ground plane or with two holes etched on the ground plane is having broader bandwidth from 4.8 GHz - 10.4 GHz with -20 dB attenuation in stopband that is there is slight increase in bandwidth and stop band attenuation as well.

As the Defected microstrip structure is causing increase of attenuation in the stop band, therefore the attenuation in the stopband is increased on increasing the number of DMS structure.

A bandstop filter with two Defected microstrip structure shows attenuation of -25 dB in Fig 3.13 while a bandstop filter with four Defected Microstrip structure provides stopband attenuation of -30 dB in Fig 3.14 with slight increase in stop bandwidth (in MHz) from 4.41 GHz - 10.4 GHz. Therefore, the more is the attenuation in the stop band the more ideal is the filter behavior.

3.5 Conclusion

A wide stopband with large attenuation greater than -30 dB is achieved by using Defected Microstrip Structure which thereby reduces copper area hence reduces cost and behaves as a more ideal filter whereas the bandwidth is enhanced by making Defects in the ground plane.

- The above results have been presented at ***47th Symposium on Modern Information and Communication Technologies for Digital India*** on 9-10, April 2016 at CSIR-CSIO Chandigarh.

Chapter 4

Dual Taylor tapered Microstrip Filter Structure employing EBG

4.1 Introduction

In this chapter, a novel small size EBG structure employing a Taylor distribution for uniform spaced antenna arrays is used to eliminate ripples in the stopband. In comparison to the Dolph - Tschebysheff array design, the Dolph - Tschebyscheff array design yields minor lobes of equal intensity while the Taylor produces a pattern whose inner minor lobes are mainly aimed at a constant level and remaining ones decrease monotonically.

4.2 Filter Design

The structure comprises of a column of periodically etched holes one after the other in the ground plane and the other plane consists of a modulated microstrip line above the substrate. The CST Microwave studio 2014 is used to simulate the proposed structure. The structure comprises of a modulated Microstrip line having five square patches above the substrate and six periodically etched holes in the ground plane.

The ratio of r and a1 is set to be 0.25. Hence the radius of etched circle is set as 2.59 mm. The total length l and the total width w is taken as 70 mm and 26 mm respectively.

Table 4.1 Specifications of Taylor Tapered BSF

Variables	Specifications
f_c (central frequency)	10 GHz
H(height of substrate)	0.762 mm
Period of EBG	10.35 mm
W	2.29 mm
Substrate	Taconic
l_a	5 mm
w_a	5 mm
R	2.59 mm
L	70 mm
W	26 mm
Filling Factor(r/a1)	0.25 mm

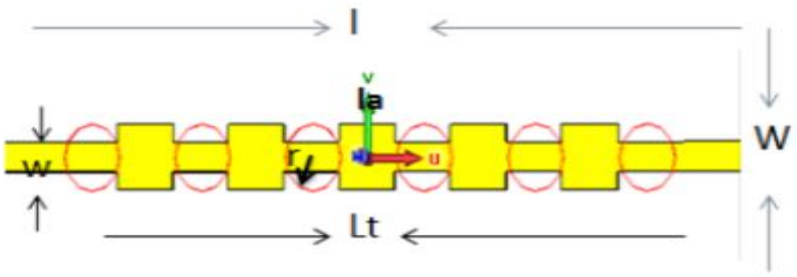

Fig. 4.1 Array of Patches etched on Microstrip line

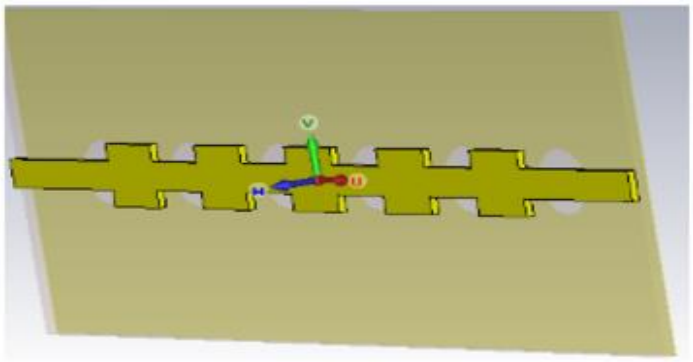

Fig. 4.2 3-D view of EBG Structure

In 2005, Several Tapering Functions like Hamming, Hanning, Bartlett, Chebyshev, Binomial, Kaiser, Gaussian, Welch, Connes, Blackman, and Cosine have been used in order to minimize ripples. But in the proposed Structure, Taylor tapering has been used which causes smooth passband and increases side lobe level.

The period a_1 is given by the distance between the adjacent centres of the circles/patches. According to the Bragg reflection condition, the period is given as:

$$\beta * a_1 = \pi \tag{4.1}$$

where,

β is the waveguide number and is described by the following equation:

$$\beta = \frac{2*\pi}{\lambda_g} \tag{4.2}$$

$$\lambda_g = \frac{c}{f_0\sqrt{\varepsilon_{eff}}} \tag{4.3}$$

$$a_1 = \frac{\lambda_g}{2} \tag{4.4}$$

4.3 Tapering Technique:

Tapering is done to eliminate ripples in the passband. In this structure, Taylor distribution of

uniform array is adopted.

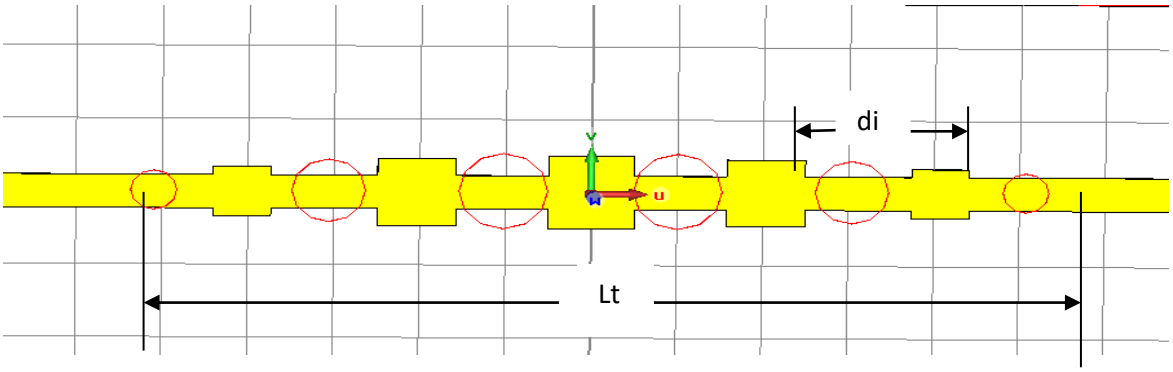

Fig. 4.3 Taylor tapered Array of Patches and holes

$$z_i = \frac{2*d_i}{Lt} \tag{4.5}$$

$$T(z_i) = J[\ j\ \pi\ B \sqrt{1 - (\frac{2*\ d_i}{L_t})^2}\ ] \tag{4.6}$$

$$L_t = [(5*(\text{length of patch})) + (6*(\text{diameter of hole}))] \tag{4.7}$$

Table 4.2 SLL vs B factor

SLL(MAX)	-10	-15	-20	-25	-30	-35
B	j0.4597	0.3558	0.7386	1.0229	1.2762	1.5136

Where

d_i : Distance between i^{th} patch and the centre of microstrip line.

z_i : Normalised distance between center of i^{th} patch and central point of microstrip structure.

L_t : Length of microstrip to taper.

The fraction of Major lobe to Minor lobe is fixed as 25 dB; therefore the normalized coefficients T (z) for patch are calculated as 1, 0.835 and 0.454. The dimension of patch adopts the following expression:

$$b_i = b_c * T(z_i) \tag{4.8}$$

b_i: Area of i^{th} patch.

b_c: Area of central circle or patch.

$$l_i^2 = l_c^2 * T(z_i) \tag{4.9}$$

$$l_i = \sqrt{l_c^2 * T(z_i)} \quad (4.10)$$

$l_1 = l_c$

$w_1 = w_c$

As the shape of patch is square, therefore the length is equal to width.

l_c and w_c of the central patch are both equal to 5 mm. Therefore l_2 , w_2, l_3 and w_3 are calculated as 4.568 mm, 4.4568 mm, 3.368 mm, 3.368 mm respectively.

Similar is the case of hole i.e.

$$z_i = \frac{2*d_i}{Lt} \quad (4.11)$$

$$T(z_i) = J[\, j\, \pi\, B \sqrt{1 - (\frac{2* d_i}{L_t})^2}\,] \quad (4.12)$$

$$L_t = [(5*(\text{length of patch})) + (6*(\text{diameter of hole}))] \quad (4.13)$$

The dimension of the hole adopts the following equation:

$$b_i = b_c * T(z_i) \quad (4.14)$$

b_i: Area of i^{th} hole.

b_c: Area of central hole.

$$\pi * r_i^2 = \pi * r_c^2 * T(z_i) \quad (4.15)$$

$$r_i = \sqrt{r_c^2 * T(z_i)} \quad (4.16)$$

r_c = 2.59 mm.

The normalized coefficients T(z) for hole are calculated as 1, 0.687 and 0.269 and hence the radius from the leftmost circle to the rightmost is 1.21 mm, 2.146 mm, 2.59 mm, 2.59 mm, 2.146 mm, 1.21 mm.

4.4 Comparison of the Uniform EBG with the proposed structure:

S11 of UNIFORM EBG

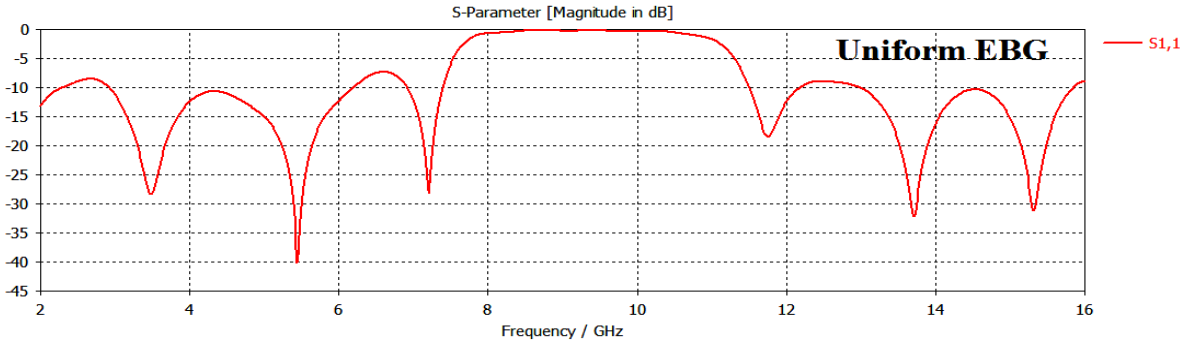

Fig. 4.4 Simulated S_{11} parameters of 2-D uniform EBG microstrip structure

SLL (Side lobe level) in the lower Passband of uniform EBG is -7 dB and ripple level is -1.2 dB whereas the SLL in the higher Passband is -10 dB.

S11 of Taylor Tapered EBG

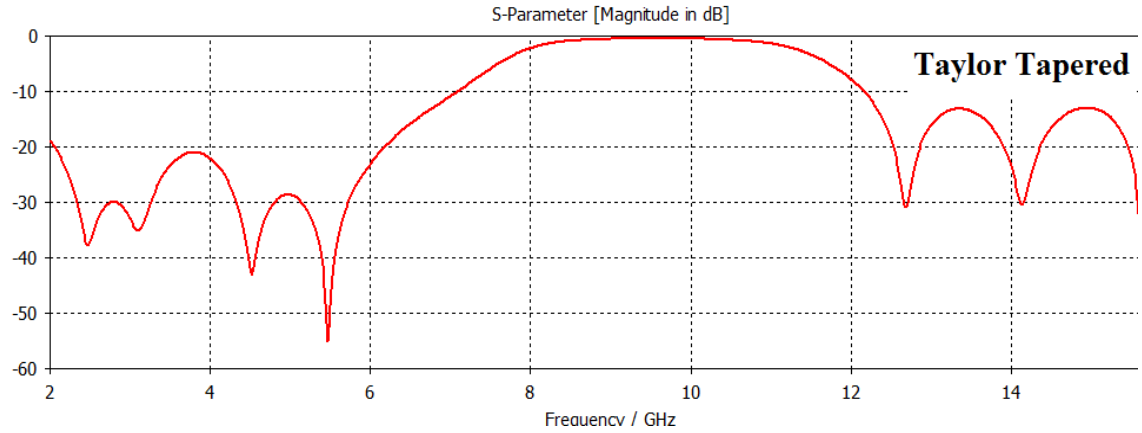

Fig. 4.5 Simulated S_{11} parameters of 2-D Taylor Tapered EBG Microstrip structure

The SLL of Taylor tapered EBG Structure in the lower Passband is found out to be -20 dB whereas the SLL in the higher Passband is found out to be -13 dB.

S21 of UNIFORM EBG

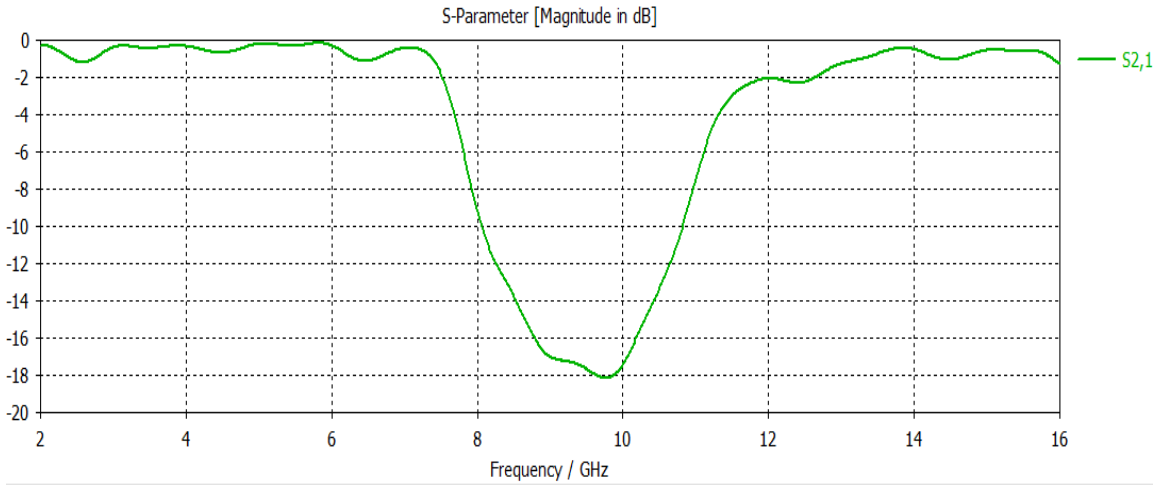

Fig. 4.6 Simulated S_{21} parameters of 2-D uniform EBG Microstrip structures

The Stop bandwidth of Uniform EBG is found as 8.06 GHz to 10.82 GHz and the Stopband attenuation is found as -18 dB. The ripple level in the lower passband is found to be -1.2 dB whereas the ripple level in the higher passband is found to be -2 dB.

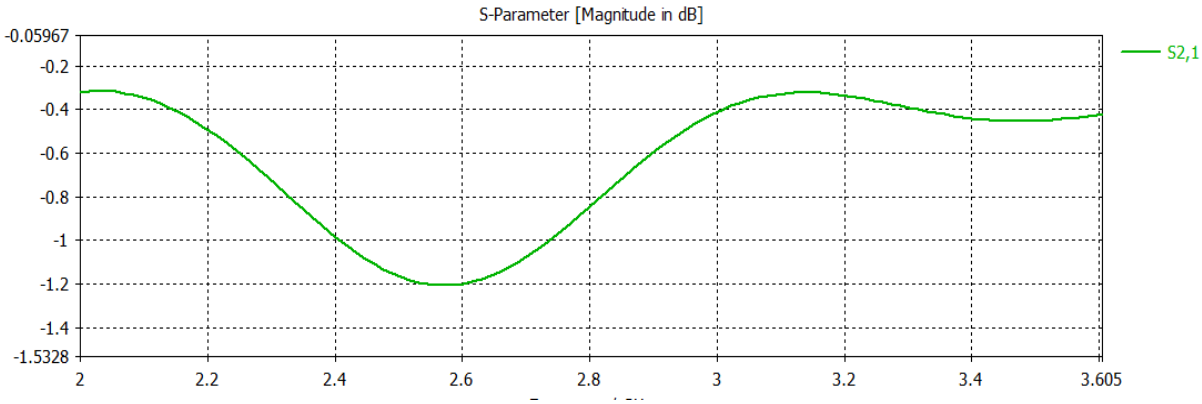

Fig. 4.7 Magnified S_{21} parameters of 2-D uniform EBG Microstrip structures

Observed Ripple level is approx. -1.2 dB in the lower passband.

S21 of Proposed Taylor Tapered EBG

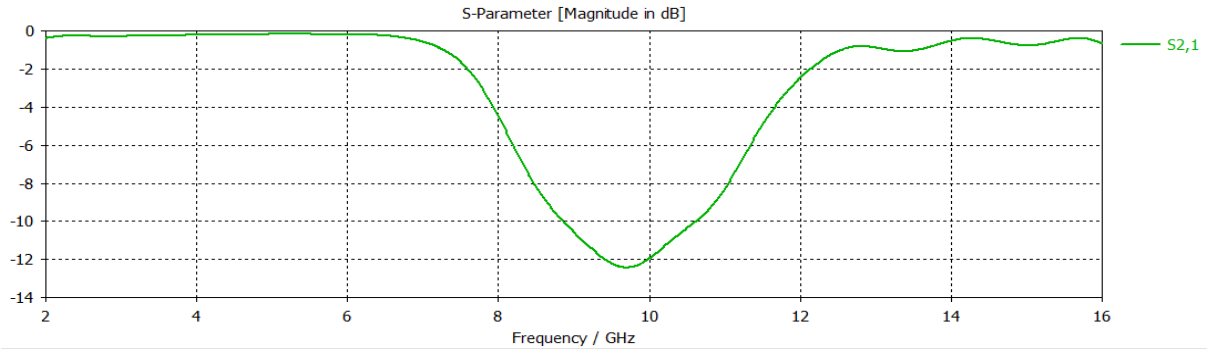

Fig. 4.8 Simulated S_{21} parameters of Taylor Tapered EBG Microstrip structures

The Stopband width of Taylor tapered EBG Structure is found as 8.86 GHz to 10.61 GHz. whereas the Stopband attenuation is found as -12.5 dB.

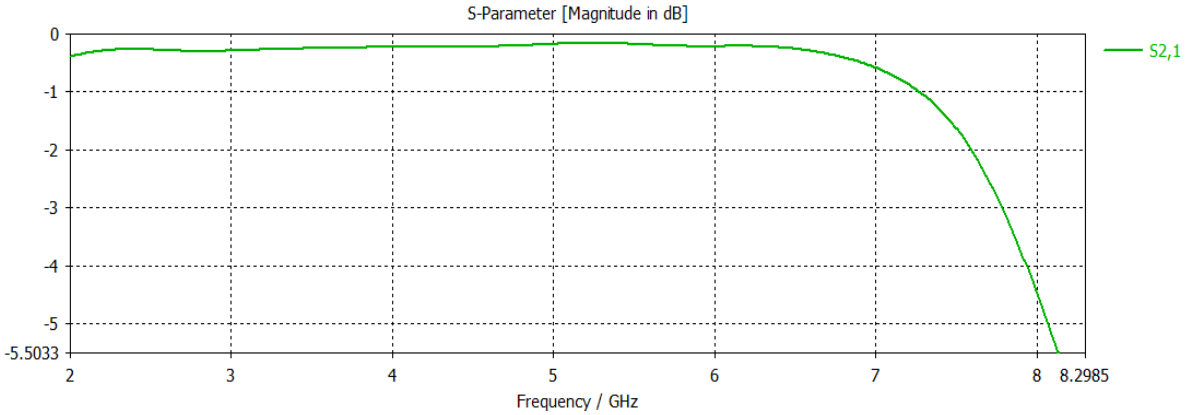

Fig. 4.9 Magnified S_{21} parameters of Taylor Tapered EBG Microstrip structures

A very flat Passband is observed in case of Taylor Tapered EBG Structure whereas large ripples upto -1.2 dB are observed in case of Uniform Structure in the lower passband. Also, the ripple level in the higher passband gets reduced from -2 dB to -1 dB.

4.5 Conclusion

It has been observed that Taylor distribution for uniform spaced antenna arrays has been used to reduce the ripple level and to increase the side lobe level with a very fine passband performance but on account of it; it has compromised the attenuation in the stop band. The following is the comparison table of Uniform distribution and the Taylor Tapered EBG.

Table 4.3 Comparison of Results of Uniform and Taylor Tapered EBG

Uniform	**Taylor Tapered**
SLL in lower passband : -8 dB	SLL in lower passband : -20 dB
Ripple level in the lower passband: -1.2 dB	A very smooth passband
Ripple level in the higher passband: -2 dB	Ripple level in the higher passband: -1 dB

- The above results are published in **International Workshop on Antenna Innovations & Modern Technologies (Iaim-2015) for Satellite Communications, Navigations & Remote Sensing Systems**.

Chapter 5

A Bandpass filter for S-Band applications

5.1 Introduction

The **S-band** is a section of the microwave band of the EM spectrum. It is defined by the IEEE standard for radio waves that the S-band frequencies ranges from 2 to 4 GHz, which crosses the conventional boundary between Ultra High Frequency and Super High Frequency at 3.0 GHz. The S band is used by the surface ship radar satellite, the weather radar satellite, and by some communications satellites which are used by NASA to communicate with the International Space Station and the Space Shuttle. It can also be used for Bluetooth, Zigbee. It is used for the satellites in geosynchronous orbit and highly eccentric orbits as well as the low orbiting satellites.

5.2 Filter Design

The Structure comprises of gap coupled high pass filter and a stepped impedance low pass filter with defects in the ground plane. The highpass filter contains gap coupled capacitors between parallel patches and the inductance lines along with the mutual inductance on the upper plane and as well as on the ground plane. The series connected four parallel plate types connected in shunt with the two gap capacitances. The gap capacitance changes the location of first pole of the highpass filter.

The dumbell shape is etched on the ground plane so as to change the resonant frequency or the bandwidth. Fig. 5.1 shows the complete structure of band pass filter.

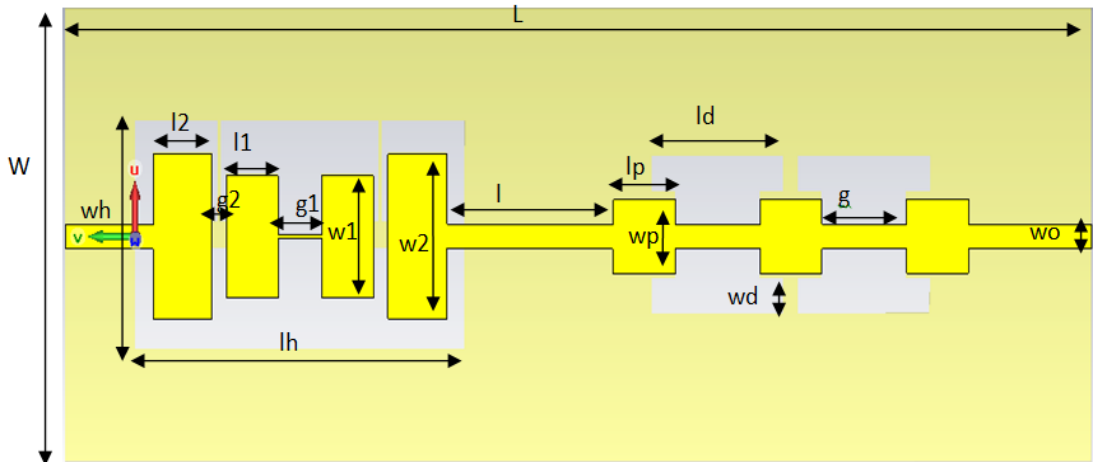

Fig. 5.1 Bandpass filter

The following are the specifications of the proposed bandpass filter.

Table 5.1 Specifications of fabricated Bandpass filter

Variables	Specifications
Substrate	FR-4
Dielectric constant	4.3
l1	3.5 mm
l2	4 mm
w1	7 mm
w2	9.45 mm
g1	3 mm
g2	1 mm
lp	4 mm
wp	4 mm
l	11 mm
g	5.5 mm
L	70 mm
W	26 mm
wo	1.5 mm
ld	9 mm
wd	2 mm
lh	22.5 mm
wh	13 mm

In this the step by step each section is analysed and then every filter section is therefore cascaded. Finally the cascaded structure's response is analysed.

5.2.1 Design of High Pass filter

Firstly a high pass filter is realized followed by the low pass filter with plane ground plane and with the dumbell shape etched on the ground plane.

The High Pass filter contains gap coupled capacitors between parallel patches and the inductance lines along with the mutual inductance based on the microstrip discontinuity. The series connected four parallel plates connected in shunt with the two gap

capacitances. The cross-coupled gap capacitance changes the location of first pole of the High Pass filter.

Fig. 5.2 shows the upper plane of a gap coupled high pass filter and Fig. 5.3 shows ground plane of a high pass filter. The width t is taken as 0.2 mm.

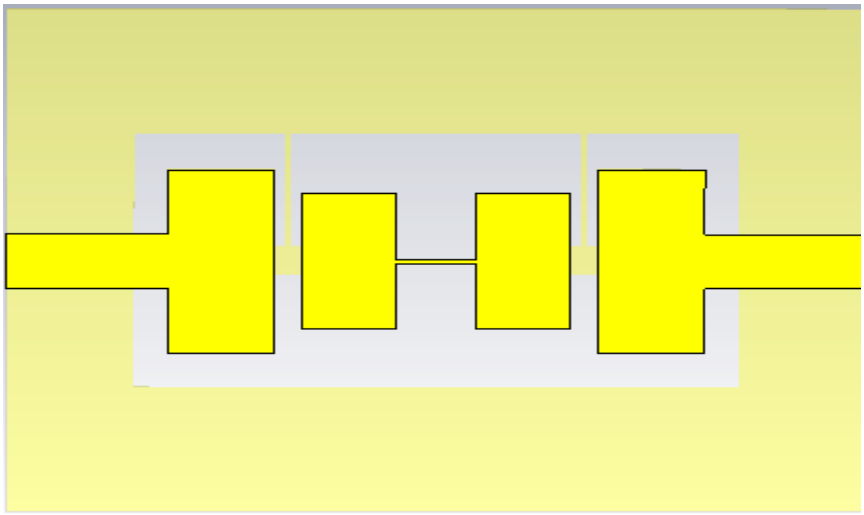

Fig. 5.2 Upper plane of a high pass filter

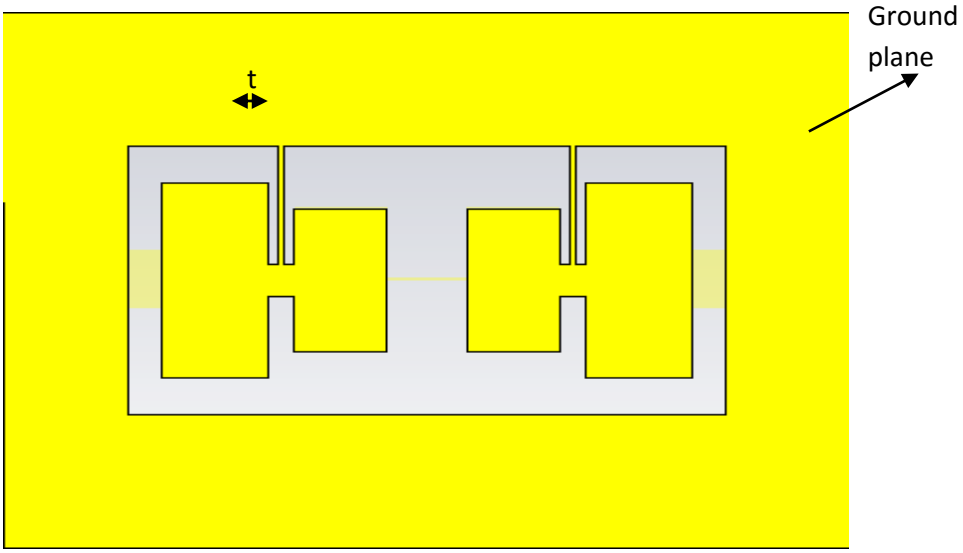

Fig. 5.3 Ground plane of a high pass filter

The following is the mathematical model including the equivalent circuit and the formulas associated with the structure.

A gap coupled high pass filter section is given as follows:

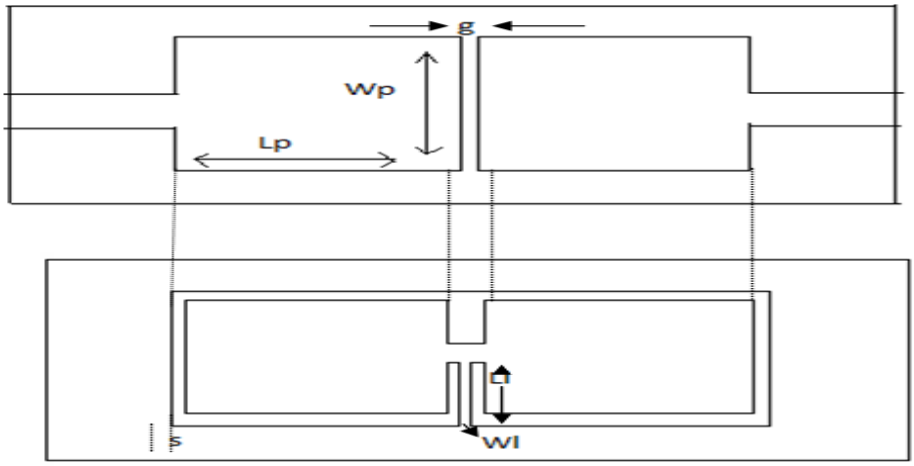

Fig. 5.4 layouts of HPF

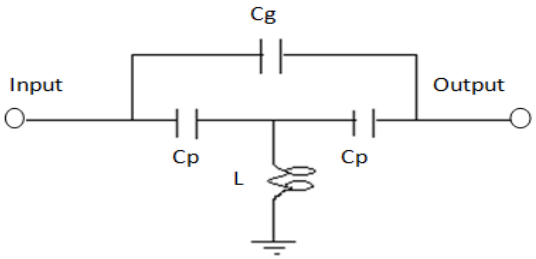

Fig. 5.5 Circuit Diagram of HPF filter

C_P is the capacitance due to parallel plate and is represented by the below formula:

$$C_P = \frac{A*\varepsilon}{h(\sim d)} \tag{5.1}$$

Where

h: is the height of Substrate

A: is the area of patch

And C_g is the gap Capacitance

The inductance L can be given as

$$L = \frac{l_m Z_m}{\lambda_g * f} \tag{5.2}$$

Where

l_m is the microstrip length

Z_m is the characteristic impedance of microstrip line

Then, the high pass filter is cascaded. Fig. 5.6 and Fig. 5.7 shows the layout and equivalent diagram of a cascaded high pass filter respectively.

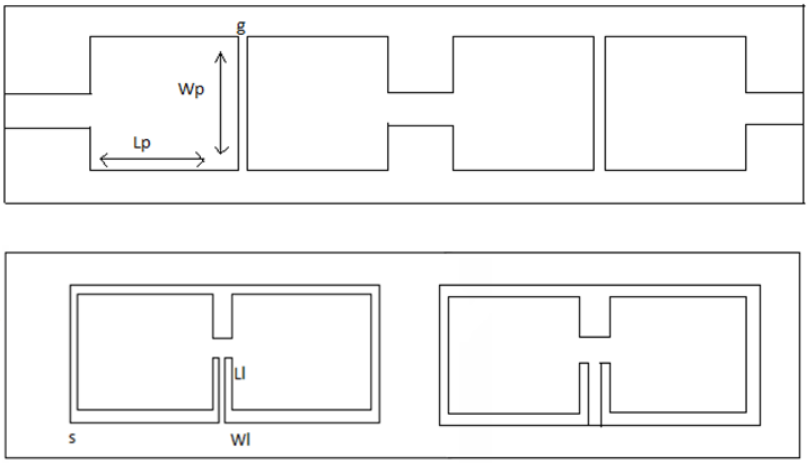

Fig. 5.6 Complete layout of cascaded High pass filter

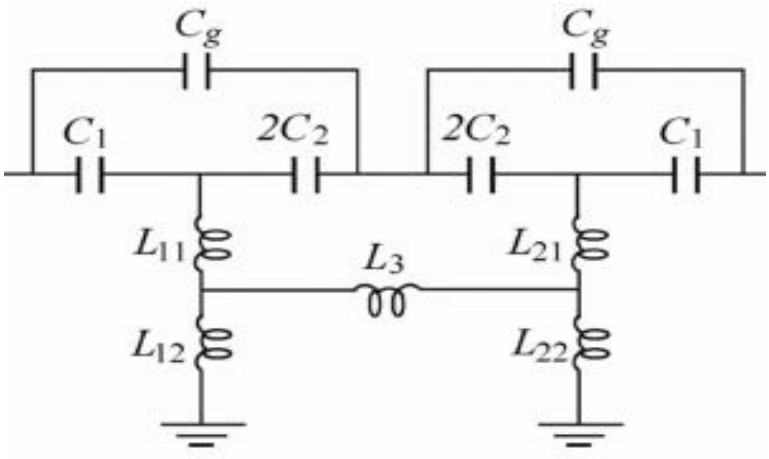

Fig. 5.7 Circuit Diagram of cascaded High pass filter

C_1 and C_2 are the parallel plate capacitors whereas

C_g is the cross coupling gap capacitance between input-output ports.

L_{11}, L_{12}, L_{21} and L_{22} are the mutual inductances.

5.2.2 Design of a low pass filter

Then a stepped impedance low pass filter is analyzed with plane ground plane followed by the ground plane etched with dumbell shape. A low pass filter comprises of a stepped impedance line. Fig. 5.8 shows the stepped impedance low pass filter with planer ground plane whereas Fig. 5.9 shows the low pass filter with dumbell shapes in the ground plane.

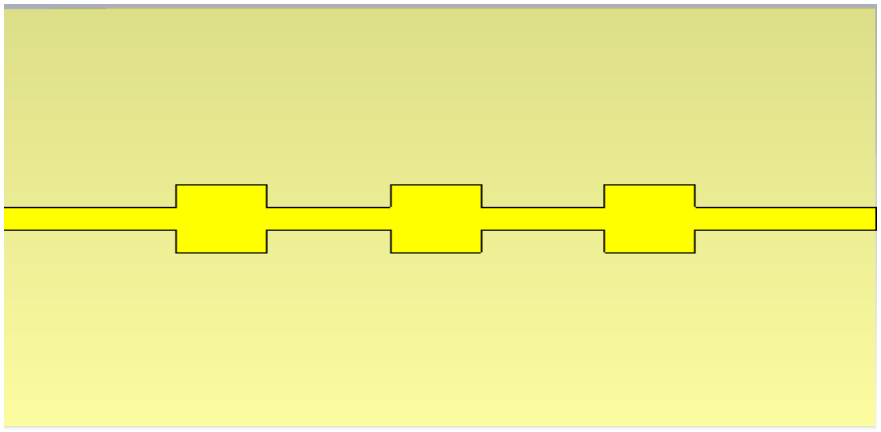

Fig. 5.8 Stepped impedance low pass filter with plane ground plane

A Stepped impedance low pass filter structure is described as follows:

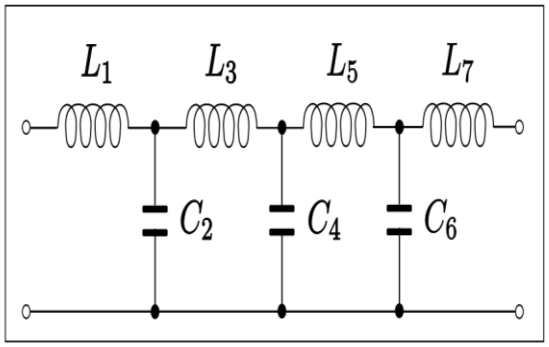

Fig 5.9 Circuit Diagram of a Low pass 7th order filter

The procedure for calculating the microstrip line length is described as below:

1. Calculate the 'A' value by using the below formula:

$$A = \frac{Z0}{60}\sqrt{\frac{\varepsilon_r+1}{2}} + \frac{\varepsilon_r - 1}{\varepsilon_r+1}\left[0.23 + \frac{0.11}{\varepsilon_r}\right] \quad (5.3)$$

2. Calculate feed width by putting the above calculated A value using the following formula:

$$\frac{w_o}{h} = \frac{8\exp(A)}{\exp(2A)-2} \quad (5.4)$$

3. Calculate the Inductance and the Capacitance value of the respective order of the filter. Here g_0 is taken as 1, g_1, g_2 and so on are calculated by the Chebyshev prototype. Taking the ripple level is equal to 0.1 dB.

Lowpass Prototype Circuit Element Values
0.1 dB equi-ripple passband amplitude Chebyshev Filter

Passband Ripple: L_{ar} = 0.1 dB; Passband Return Loss > 16dB

Prototype Elements:	g_1	g_2	g_3	g_4	g_5	g_6	g_7	g_8	g_9	g_{10}	g_{11}
Order : N	C_1	L_2	C_3	L_4	C_5	L_6	C_7	L_8	C_9	L_{10}	
1	0.30552	1.00000					g_i = Inductance for series inductors. Capacitance for shunt capacitors.				
2	0.84349	0.62216	1.35574								
3	1.03201	1.14745	1.03201	1.00000							
4	1.10923	1.30617	1.77083	0.81818	1.35574						
5	1.14726	1.37117	1.97544	1.37117	1.14726	1.00000					
6	1.16855	1.40391	2.05663	1.51698	1.90333	0.86193	1.35574				
7	1.18162	1.42273	2.09707	1.57325	2.09707	1.42273	1.18162	1.00000			
8	1.19019	1.43457	2.12029	1.60084	2.17033	1.56394	1.94491	0.87789	1.35574		
9	1.19611	1.44252	2.13494	1.61655	2.20574	1.61655	2.13494	1.44252	1.19611	1.00000	
10	1.20036	1.44811	2.14482	1.62641	2.22569	1.64168	2.20499	1.58203	1.96326	0.88539	1.35574
	L_1	C_2	L_3	C_4	L_5	C_6	L_7	C_8	L_9	C_{10}	

Fig: 5.10 Chebyshev coefficients for 0.1 dB ripple level

$$L_i = \left(\frac{Z_o}{g_o}\right)\left(\frac{\Omega_c}{2\,\pi\,f_c}\right) g_1 \tag{5.5}$$

$$C_i = \left(\frac{g_o}{Z_o}\right)\left(\frac{\Omega_c}{2\,\pi\,f_c}\right) g_2 \tag{5.6}$$

$$l_L = \left(\frac{\lambda_{gl}}{2\,\pi}\right) \sin^{-1}\left(\frac{w_c\,L_i}{Z_{oL}}\right) \tag{5.7}$$

$$l_c = \left(\frac{\lambda_{gc}}{2\,\pi}\right) \sin^{-1}\left(\frac{w_c\,C_i}{Z_{oc}}\right) \tag{5.8}$$

By using these equations, the length of the patches is calculated as 4 mm and the length between the patches is calculated as 5.5 mm for the frequency 5.5 GHz of a low pass filter.

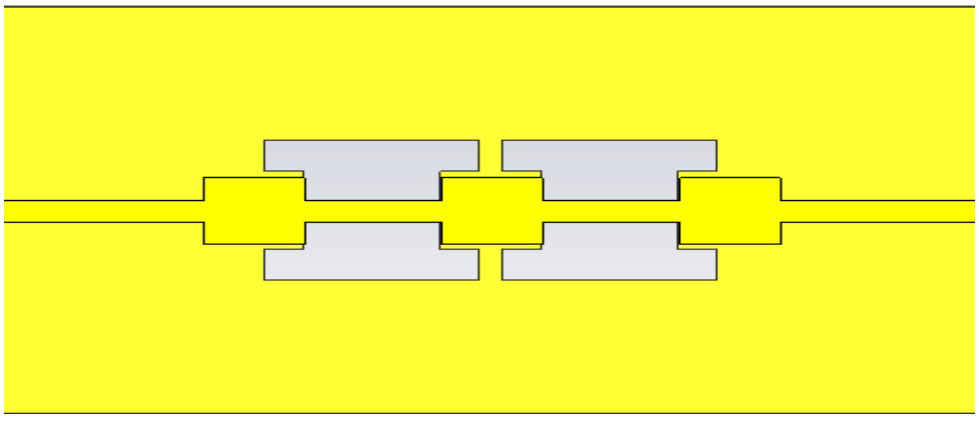

Fig. 5.11 Stepped impedance low pass filter with dumbell slots in the ground plane

5.2.3 Cascading of High Pass and a Low Pass filter

Fig. 5.12 shows the bandpass filter for S-band without dumbell slots while the Fig. 5.13 shows the complete bandpass filter with dumbell slots.

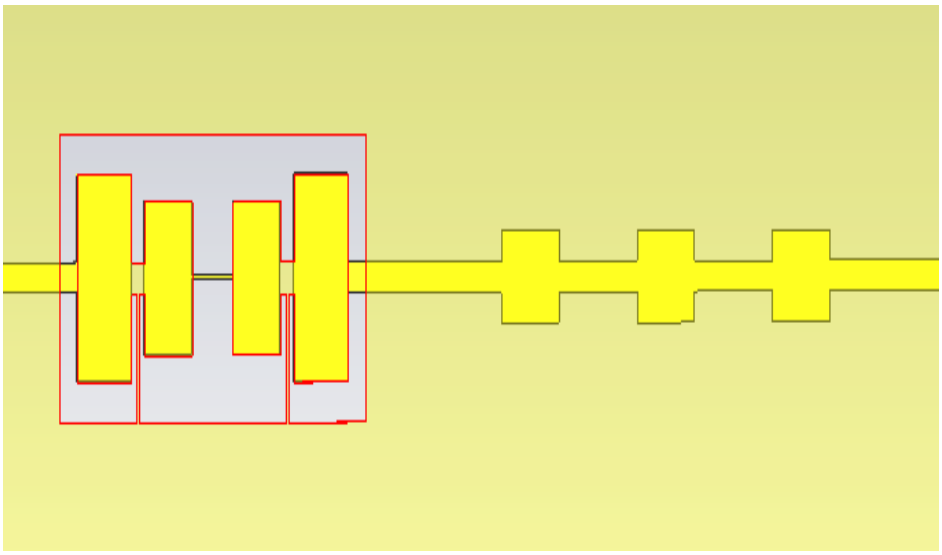

Fig. 5.12 A Band Pass Filter without dumbell slots

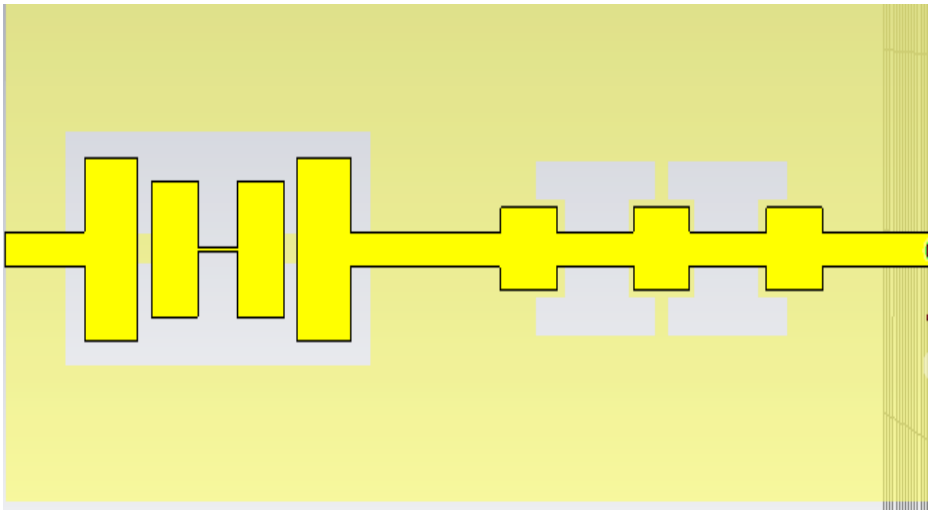

Fig. 5.13 A Complete Band Pass Filter

5.3 Simulated Results

The results of a Bandpass Filter using EBG structure design in terms of the insertion loss and the return loss have been obtained by using the CST Microwave Studio 2014 software. The proposed filter with optimal parameters is shown above and their respective results have been described below.

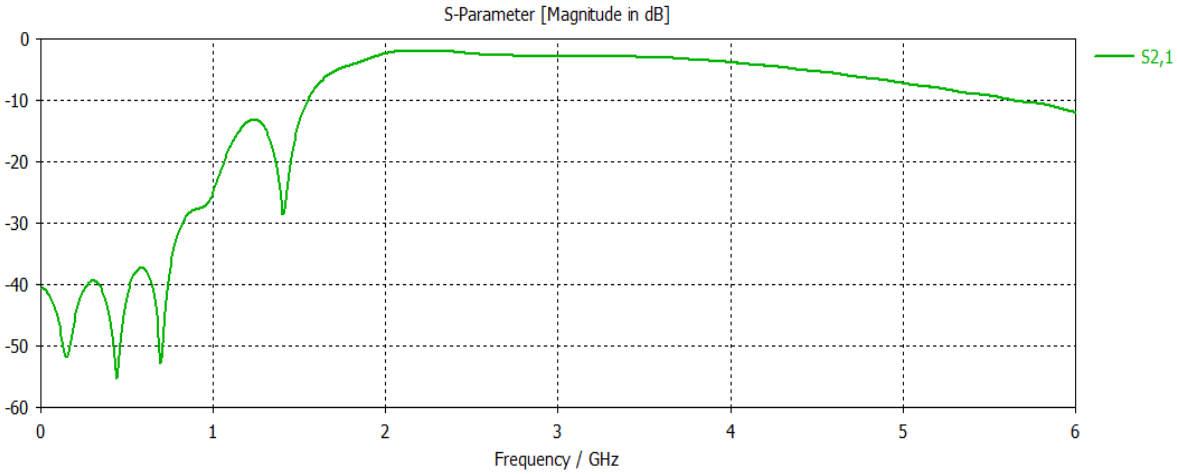

Fig. 5.14 S21 of a High pass filter

The above figure shows the S21 parameters of high pass filter in which the 0 dB cut off frequency is 2 GHz. And now the high pass filter is cascaded with the low pass filter to form a bandpass filter. Fig. 5.15 shows the simulated results of a low pass filter with a planer ground plane whereas Fig. 5.16 shows the simulated results of low pass filter with defects in the ground plane.

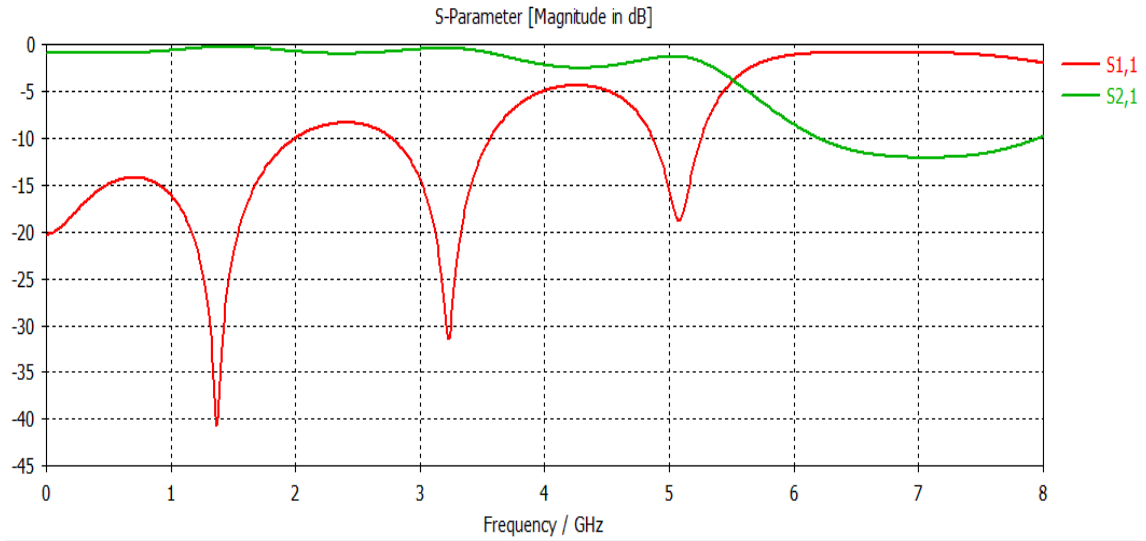

Fig. 5.15 Simulated results of a low pass filter with planer Ground plane

5.4 Effect of dumbell slots on the ground plane

It has been observed from the above and the below figure that the dumbell slots introduces some additional inductance and capacitance which alters the resonant frequency and thereby the bandwidth also gets affected. The low pass filter with planer ground plane is having 10 dB cut off frequency at 6 GHz and a 0dB cut off frequency at

5Ghz whereas the low pass filter with defects in the ground plane in the below figure is having 0 dB cut off frequency at 4 GHz and a 10 dB cut off frequency at 4.3 GHz.

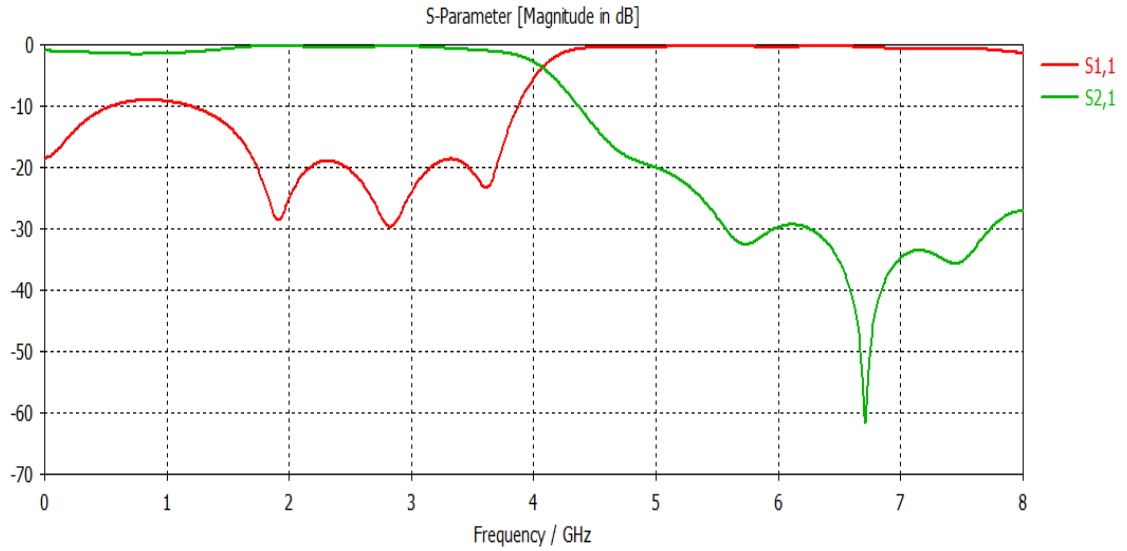

Fig. 5.16 Simulated Results of a low pass filter with dumbell slots etched on the ground plane

Fig. 5.17 shows the simulated results of a bandpass filter without dumbell slots. The low pass response in the following figure is almost similar to the low pass filter without dumbell slots. So, in order to make the filter to give a low pass response only less than and equal to 4 Ghz the dumbell slots are etched in the ground plane.

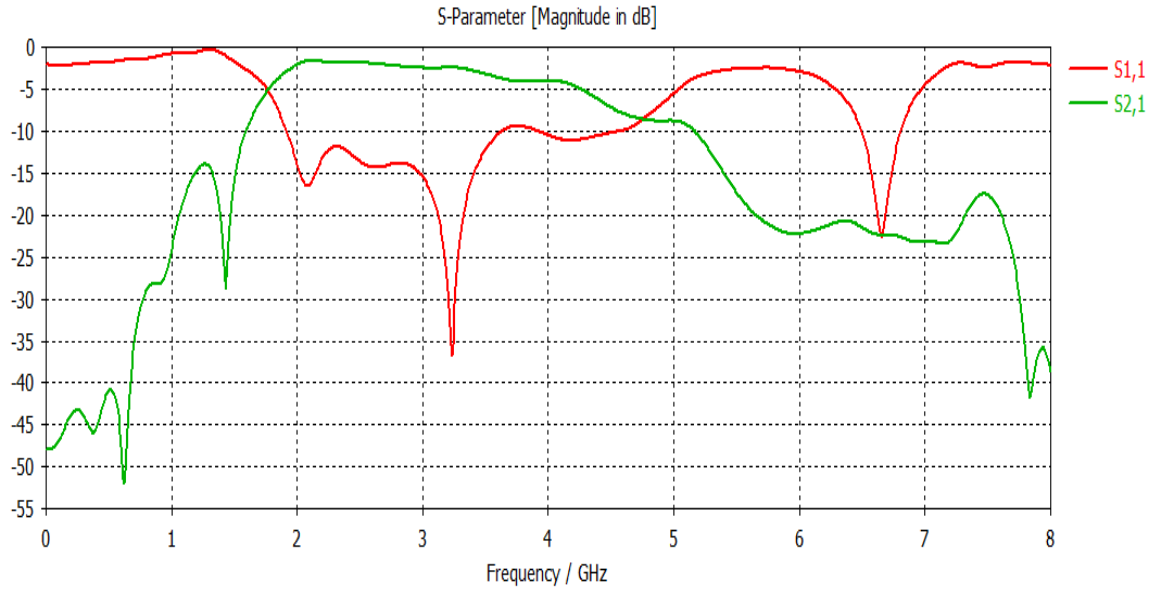

Fig. 5.17 Simulated results of a bandpass filter without dumbell slots

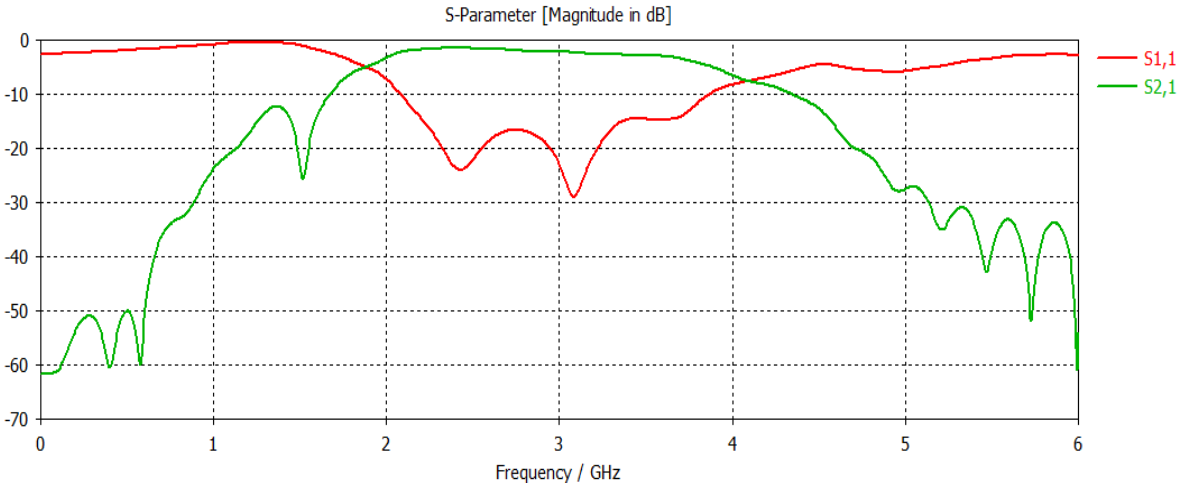

Fig. 5.18 Simulated Results of a complete Band Pass filter

Fig. 5.18 shows simulated results of the final bandpass filter which is having bandwidth from 2 GHz from 4 GHz which can be used for the S-band applications. The SLL in the lower band is -13 dB whereas the SLL in the higher band is -30 dB.

5.5 Fabricated Band Pass Filter and Measured Results

The simulated filter is fabricated using FR-4 substrate with dielectric constant 4.4, tanδ = 0.0024 and a thickness of 1.6 mm. The thickness of the copper is taken as 0.035 mm. The return loss and the insertion loss of the fabricated filter are tested with the help of Agilent E5071C vector network analyzer available at Antenna Research Laboratory, Thapar University, Patiala.

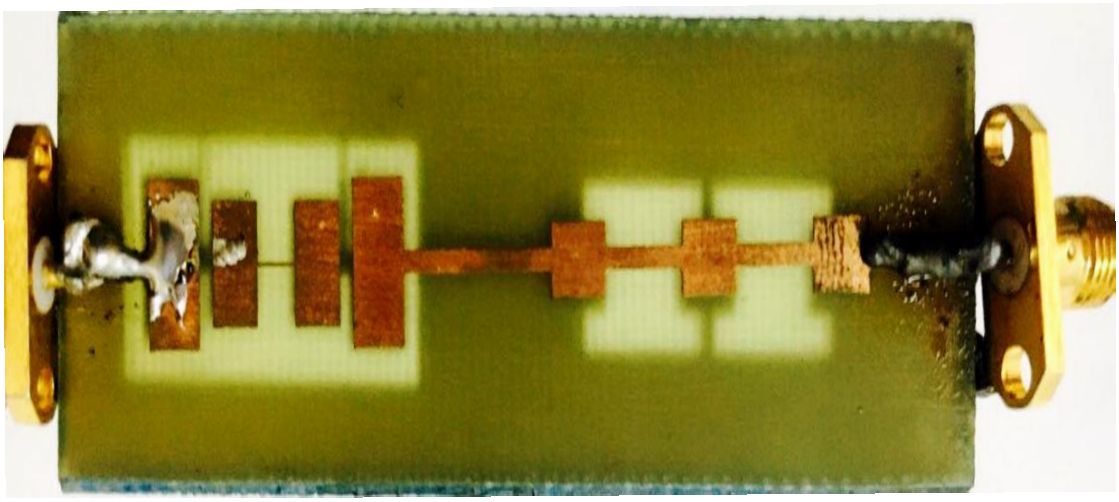

Fig. 5.19 Top view of the fabricated Band Pass filter for S-Band applications

Fig. 5.20 Bottom view of the fabricated Band Pass filter for S-Band applications

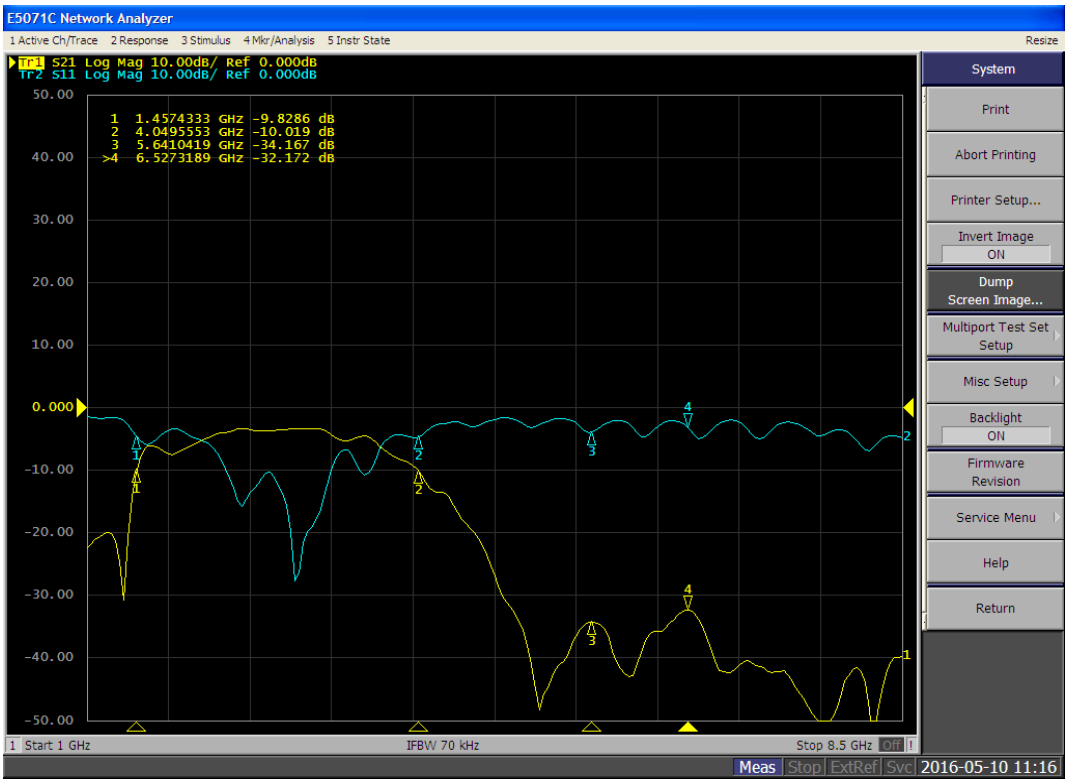

Fig. 5.21 Measured Results of a fabricated filter structure

The observed frequency band is from 1.45 GHz to 4.02 GHz in the measured eresults. This band is used for the S-Band applications. The slight disagreement between simulated and fabricated results of the designed filter could be attributed due to the fabrication errors, mismatch between SMA connector and feeder, noise and interference etc.

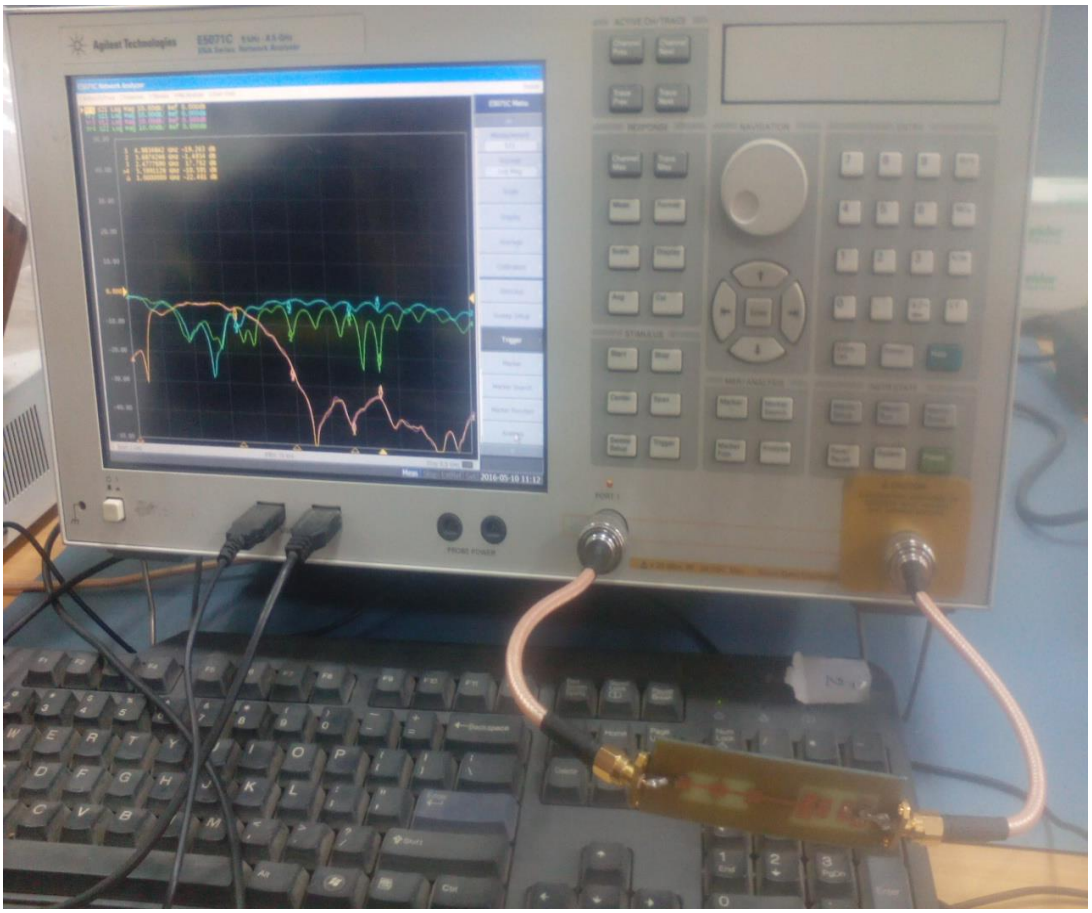

Fig 5.22 Filter testing on VNA

5.6 Conclusion

The high pass and a low pass filters are cascaded to obtain bandpass filter response which is giving frequency response from 2 to 4 GHz which can be used for the S-Band applications. The gap capacitance changes the location of first pole of the highpass filter whereas the low pass resonant frequency slightly gets changed due to the dumbell shape etched on the ground plane. Because the filter covers complete S-Band (2-4GHz), therefore it can be used in the domains of Bluetooth, LTE, WiMAX, HSDPA, WLAN applications but in future, work can be done to improve its return loss and the structure can be miniaturized.

- The above results have been communicated to **Indian Journal of Science and Technology.**

Chapter 6

Conclusion and Future Scope

6.1 Conclusion

The main aim of the entire thesis was to design a Microstrip Filter employing Electromagnetic Bandgap with large SLL, low ripple level, smooth passband and a large attenuation in the stopband.

From the Chapter 3, it was concluded that the defects in the Microstrip structure also puts a great role in achieving large attenuation in the stopband. On increasing the number from zero to symmetric two to symmetric four DMS, the attenuation increases from -20 dB to -25 dB and then to -30 dB.

From the Chapter 4, it was concluded that the dual Taylor Tapered Microstrip Filter Structure was able to achieve a very smooth passband on comparison with the Uniform EBG. It has been observed that Taylor distribution for uniform spaced antenna arrays has been used to reduce the ripple level and to increase the side lobe level with a very fine passband performance but on account of it; it has compromised the attenuation in the stop band.

From the Chapter 5, it was concluded that the gap capacitance changes the location of first pole of the highpass filter whereas the low pass resonant frequency slightly gets changed due to the dumbell shape etched on the ground plane. Because the filter covers complete S-Band (2-4GHz), therefore it can be used in the domains of Bluetooth, LTE, WiMAX, HSDPA, WLAN applications but it suffers from poor return loss.

6.2 Future Scope

- The stepped impedance filters can be used to control the Bandwidth also.
- In future, work can be done to improve the return loss.
- The structure can be miniaturized.

References

[1] F. Yang and Y. R. Samii, "Electromagnetic Band Gap Structures in Antenna Engineering," in Cambridge University Press 2009.

[2] E. Yablonovitch, "Inhibited Spontaneous Emission in Solid-State Physics and Electronics," *Physics Rev. Letters*, vol. 58, no. 20, pp. 2059-2062, May 1987.

[3] S. John, "Strong Localization of Photons in Certain Disordered Dielectric Super Lattices," *Physics Rev. Letters*, vol. 58, no. 23, pp. 2486-2489 , June 1987.

[4] H. Kogelnik and C.V. Shank, "Coupled Wave Theory of Distributed Feedback Lasers," *Journal of Applied Physics*, vol. 43, no.5, pp. 2327-2335, May 1972.

[5] A. Yariv, P. Yeh, "Optical Waves in Crystals," Wiley & Sons, 1984.

[6] Ramesh Garg and Prakash Bhartia, Inder Bahl, Apisak Ittipiboon, "Microstrip antenna design Handbook," Artech House, inc. Norwood, 2001.

[7] Harish Kumar, Manish Kumar, Mohit Kumar and Rajeev Kanth, "Study on Band Gap Behaviour of Electromagnetic Band-Gap(EBG) Structure With Microstrip Antenna," *International Conference on advanced Communication Technology*, pp. 356-359, Feb. 2012.

[8] Alka Verma, "Ebg Structures And Its Recent Advances In Microwave Antenna," *International Journal of Scientific Research Engineering & Technology*, vol. 1, no. 5, pp. 84-90, Aug. 2012.

[9] Steve Winder and Joseph Carr, "Radio and R.F Engineering Pocket Book," 3rd ed., Great Britain, pp. 2-3, 2002.

[10] D.M. Pozar, "Microwave engineering," 3rd ed., pp. 389-410, 2005.

[11] Hua Zhang, Hongmin LU and Zhenxing Wan, "Ultra-wideband SSN suppression using novel Electromagnetic Band-gap Structures," *International Symposium on Antennas Propagation and EM Theory*, pp. 686-688, Dec. 2010.

[12] Abou Hussein and Rammal Mohamed, "1D Ultra Low-Profile (ULP) EBG Matrix for Radar Applications," *IEEE Conference on Radar*, pp. 1-4, May 2013.

[13] Z.Z Abidin, Y. Ma, R. A. Abd-Alhameed, K. N. Ramli , D. Zhou, M. S. Bin-Melha, J. M. Noras, and R. Halliwell, "Design of 2 x 2 U-shape MIMO slot antennas with EBG material for mobile handset applications," *Piers Online*, vol. 7, no. 1, pp. 81-84, 2011.

[14] John D. Shumpert, William J. Chappell and Linda P. B. Katehi, "Parallel-Plate Mode Reduction in Conductor-Backed Slots Using Electromagnetic Bandgap

Substrates," *IEEE Transactions on Microwave Theory and Techniques*, vol. 47, no. 11, pp. 2099-2104, Nov. 1999.

[15] Shau-Gang Mao and Ming-Yi Chen, "A Novel Periodic Electromagnetic Bandgap Structure for Finite-Width Conductor-Backed Coplanar Waveguides," IEEE *Microwave and Wireless Components Letters*, vol. 11, no. 6, pp. 261-263, June 2001.

[16] Joan Garcia-Garcia, Jordi Bonache and Ferran Martin, "Application of Electromagnetic Bandgaps to the Design of Ultra-Wide Bandpass Filters with Good Out-of-Band Performance," *IEEE Transactions on Microwave Theory and Techniques*, vol.54, no.12, pp. 4136-4140, Dec. 2006.

[17] William J. Chappell, Matthew P. Little and Linda P. B. Katehi, "High Isolation, Planar Filters Using EBG Substrates," *IEEE Microwave and Wireless Components Letters*, vol. 11, no. 6, pp. 246-248, June 2001.

[18] Yasushi Horii and Makoto Tsutsumi, "Wide Band Operation of a Harmonically Controlled EBG Microstrip Patch Antenna," *IEEE International Symposium on Antennas and Propagation society*, vol. 3, pp. 768-771, June 2002.

[19] Hsiuan-ju Hsu, Michael J. Hill, John Papapolymerou, and Richard W. Ziolkowski, "A Planar X-Band Electromagnetic Band-Gap (EBG) 3-Pole Filter," *IEEE Microwave and Wireless Components Letters*, vol. 12, no. 7, pp. 255-257, July 2002.

[20] C.C. Chiau, X. Chen and C. Parini, "Multiperiod EBG structure for wide stopband circuits," *IEEE Proceedings on Microwave Antennas and Propagation*, vol. 150, no. 6, pp. 489-492, Dec. 2003.

[21] M.F. Karim, A.Q. Lieu, A. Alphones and X.J Zhang, "Low Pass Filter using a Hybrid EBG," *IEEE Microwave and Optical Technology Letters*, vol. 45, no. 2, pp. 95-98, April 2005.

[22] Shao Ying Huang and Yee Hui Lee, "Tapered Dual Plane Compact Electromagnetic Bandgap Microstrip Filter Structures," *IEEE Transactions on Microwave Theory and Techniques*, vol. 53, no. 9, pp. 2656-2664, Sept. 2005.

[23] Shao Ying Huang and Yee Hui Lee, "Compact U-Shaped Dual Planer EBG Microstrip Low-pass Filter," *IEEE Transactions on Microwave Theory and Techniques*, vol. 53, no. 12, pp. 3799-3805, Dec 2005.

[24] M. F. Abedin, M. Z. Azad, and M. Ali, "Wideband Smaller Unit-Cell Planar EBG Structures and Their Application," *IEEE Transactions on Antennas And Propagation*, vol. 56, no. 3, pp. 903-908, March 2008.

[25] Jung-Woo Baik, Sang-Min Han, Chandong Jeong, Jichai Jeong and Young-Sik Kim, "Compact Ultra-Wideband Bandpass Filter With EBG Structure," *IEEE Microwave And Wireless Components Letters*, vol. 18, no. 10, pp. 671-673, Oct. 2008.

[26] Dong-Jin Jung and Kai Chang, "Low-Pass Filter Design through the accurate analysis of Electromagnetic-Bandgap Geometry on the Ground Plane," *IEEE Transactions on Microwave Theory and Techniques*, vol. 57, no. 7, pp. 1798-1805, July 2009.

[27] Lin Peng, Cheng-li Ruan and Zhi-Qiang Li, "A Novel Compact and Polarisation-Dependent Mushroom-Type EBG Using CSRR for Dual/Triple-Band Applications," *IEEE Microwave and Wireless Components Letters*, vol. 20, no. 9, pp. 489-491, Sept. 2010.

[28] B.-W Lieu, Y.-Z. Yin, Y. Yang, S.-H Jing and A.-F Sun, "Compact UWB Bandpass Filter with two notched bands based on electromagnetic bandgap Structures," *IET Electronics Letters*, vol. 47, no. 3, pp. 757-758, June 2011.

[29] Sang il Kwak, Dong-Uk Sim, and Jong Hwa Kwon, "Design of Optimized Multilayer PIFA with the EBG Structure for SAR Reduction in Mobile Applications," *IEEE Transactions on Electromagnetic Compatibility*, vol. 53, no. 2, pp. 325-331, May 2011.

[30] Lin Peng, Cheng-li Ruan and Jiang Xiong, "Compact EBG for Multiband applications," *IEEE Transactions on Antennas and Propagation*, vol. 60, no. 9, pp. 4440-4444, Sept. 2012.

[31] Haoran Zhu and Junfa Mao, "Miniaturized Tapered EBG Structure with Wide Stopband and Flat Passband," *IEEE Antennas and Wireless Propagation Letters*, vol. 11, pp. 314-317, April 2012.

[32] Chen Fei Su, Xing Qun Qi and Zheng Bo Yang, "Design of UWB Bandpass Filter Using Highpass and Dual-Plane EBG Lowpass Filters," *Proceedings IEEE International Conference on Applied Superconductivity and Electromagnetic Devices*, pp. 149-152, Oct. 2013.

[33] D. Sridhar Raja, "Periodic EBG Structure Based UWB Bandpass Filter," *International Journal of Advanced Research in Electrical, Electronics and Instrumentation Engineering*, vol. 2, pp. 1682-1686, May 2013.

[34] Myunghoi Kim, Kyoungchoul Koo, Yujeong Shim, Chulsoon Hwang Jun So Pak, Seungyoung Ahn and Joungho Kim, "Vertical Stepped Impedance EBG (VSI-EBG) Structure for Wideband Suppression of Simultaneous Switching Noise in Multilayer PCBs," *IEEE Transactions on Electromagnetic Compatibility*, vol. 55, no. 2, pp. 307-314, April 2013.

[35] Zhaowen Yan, Yin Xiong, Wenlu Yu and Yansheng Wang, "An Improved Miniatuzised Three-Layer Embedded Electromagnetic Bandgap Structure," *IEEE Transactions on Antennas and Propagation*, vol. 62, no. 5, pp. 2832-2837, May 2014.

[36] Pooja Sahoo and P.K Singhal , "Design of new compact Photonic Bandgap Filter and their Advantages," *International Journal of Electronics and Electrical Engineering*, vol. 3, no. 2, pp. 84-88, April 2014.

[37] Wengang Chen, Constantine A. Balanis and Craig R. Birtcher, "Checkerboard EBG Surfaces for Wideband Radar Cross Section Reduction," *IEEE Transactions on Antennas and Propagation*, vol. 63, no. 6, pp. 2636-2645, June 2015.

[38] Jaun de Dios Ruiz, Felix Lorenzo Martinez-Viviente and Juan Hinojosa, "Optimisation of Chirped and Tapered Microstrip Koch Fractal electromagnetic Bandgap Structures for improved Low-pass Filter Design," *IET Microwaves, Antennas and Propagation*, vol. 9, pp. 889-897, June 2015.

[39] Jaun de Dios Ruiz, Felix Lorenzo Martinez-Viviente, Alejandro Alvarez-Melcon and Juan Hinojosa, "Substrate Integrated Waveguide (SIW) With Koch Fractal Electromagnetic Bandgap Structures (KFEBG) for Bandpass Filter Design," *IEEE Microwave and Wireless Components Letters*, vol. 25, no. 3, pp. 160-162, March 2015.

[40] Sai Wai Wong, Rui Sen Chen, Kai Wang, Zhi-Ning Chen and Qing-Xin, Chu, "U-Shape Slots Structure on Substrate Integrated Waveguide for 40-GHz Bandpass Filter Using LTCC Technology," *IEEE Transactions on Components, Packaging and Manufacturing Technology*, vol. 5, no. 1, pp. 128-134, Jan. 2015.

[41] Ramesh Garg, Inder Bahl and Maurizio Bozzi, "Microstrip Lines and Slotlines," 3rd edition, Artech House, 2013.

- Ambika Chhabra, Rajesh Khanna, "A DMS based Microstrip Bandstop Filter with large attenuation," presented at ***47th Symposium on Modern Information and Communication Technologies for Digital India*** on 9-10, April 2016 at CSIR-CSIO Chandigarh.
- Ambika Chhabra, Rajesh Khanna, "Dual Taylor Tapered Microstrip Filter Structure Employing Electromagnetic Band Gap," published in **International Workshop on Antenna Innovations & Modern Technologies (Iaim-2015) for Satellite Communications, Navigations & Remote Sensing Systems**.
- Ambika Chhabra, Rajesh Khanna, "A Bandpass filter for S-Band Applications," communicated to **Indian Journal of Science and Technology.**

Awards

First Best paper award at 47th Symposium on Modern Information and Communication Technologies for Digital India held on 9-10 April 2016 at CSIR-CSIO Chandigarh.

Certificate of Best Paper Award

47th Mid-Term Symposium on

Modern Information and Communication Technologies for Digital India

(MICTDI – 2016) | (APRIL 09-10, 2016)

Best Paper Award

presented to

Dr/Mr/Ms AMBIKA CHHABRA

for his/her paper entitled Miniaturized DMS Based Microstrip Bandstop Filter with Large Attenuation

authored by Ambika chhabra, Rajesh Khanna

(Surender Singh Saini)
Co-Convener

(Neelesh Kumar)
Convener

(S.K Angra)
Conference Chair

(Prof. R.K Sinha)
Conference Chair

Thesis

ORIGINALITY REPORT

6%	3%	5%	0%
SIMILARITY INDEX	INTERNET SOURCES	PUBLICATIONS	STUDENT PAPERS

PRIMARY SOURCES

1	S.Y. Huang. "Tapered Dual-Plane Compact Electromagnetic Bandgap Microstrip Filter Structures", IEEE Transactions on Microwave Theory and Techniques, 9/2005 Publication	1%
2	XiaoQun Chen. "Compact low pass filter using novel elliptic shape DGS", Microwave and Optical Technology Letters, 04/2009 Publication	1%
3	Y.H. Lee. "A novel dual-plane compact electromagnetic band-gap (DPC-EBG) filter design", ICMMT 4th International Conference on Proceedings Microwave and Millimeter Wave Technology 2004, 2004 Publication	<1%
4	Su, Chen Fei, Xing Qun Qi, and Zheng Bo Yang. "Design of UWB bandpass filter using highpass and dual-plane EBG lowpass filters", 2013 IEEE International Conference on Applied Superconductivity and Electromagnetic Devices, 2013. Publication	<1%